Marine Environmental Research 207 (2025) 107090

Contents lists available at ScienceDirect

Marine Environmental Research

journal homepage: www.elsevier.com/locate/marenvrev

Elucidating divergent growth and climate vulnerability in abalone (*Haliotis iris*): A multi-year snapshot

Joanna S. Copedo [a,b,*], Stephen C. Webb [a], Lizenn Delisle [a], Ben Knight [a], Norman L.C. Ragg [a], Olivier Laroche [a], Leonie Venter [b], Andrea C. Alfaro [b]

[a] Cawthron Institute, Nelson, 7042, New Zealand
[b] Aquaculture Biotechnology Research Group, Department of Environmental Science, School of Science, Auckland University of Technology, Private Bag 92006, Auckland, 1142, New Zealand

ARTICLE INFO

Keywords:
Haliotis iris
Abalone
Histopathology
Parasites
Gametogenesis
Atresia

ABSTRACT

Many abalone populations worldwide are in decline as a result of changing climate and fishing pressure. In New Zealand (NZ) *Haliotis iris* is the largest and most abundant of the endemic abalone species. This species displays high levels of phenotypic variation with slow-growing populations having an impact on their commercial utilisation. The present study incorporates targeted histopathological approaches to characterise tissue-level factors in abalone from NZ's principal fishing region. Adult (n = 60) and sub-adult (n = 56) *H. iris* were collected from two Chatham Island sites that display differential growth rates; sampling was repeated on six occasions over three years. Through histology the slower-growing adult population was observed to have an elevated ceroid score, higher prevalence of kidney stones and increased prevalence of a plasmodia stage of haplosporidian-like parasites in the right kidney, when compared with the faster-growing and sub-adult populations. Furthermore, the faster-growing adult population appeared to be retaining mature oocytes over the predicted spawning season with higher-than-expected atresia (oocyte degeneration). Factors implicated in growth performance between the two populations include site, environment, parasites, pathology, reproduction, ceroid deposition and previously reported nutritional status. The 18S PCR and metabarcoding on the right kidney tissue were negative for haplosporidian/*Urosporidium* previously reported in *H. iris*, with metabarcoding results detecting an apicomplexan ancestral group. The reproductive, somatic and parasite findings from the current study provides critical information on abalone physiological condition which allows facilitation of early detection of conditions that may impact the sustainability and management of *H. iris* stocks in New Zealand under a changing climate. For instance, changes to reproductive condition may reduce oocyte quality and quantity thereby reducing recruitment to the next generation.

1. Introduction

Abalone are ecologically important coastal marine gastropods from the Haliotidae family and are globally widespread (Geiger, 1999). Many abalone populations are in decline, with several nearing biological extinction (Gnanalingam et al., 2021). These declines are often attributed to over-fishing, habitat degradation, and disease (Cook, 2014; Van Nguyen et al., 2023). Additionally, the coastal ecosystems which abalone inhabit are often highly impacted by environmental alterations influenced by climate change (Halpern et al., 2008; Lima and Wethey, 2012). The influence of climate change and corresponding decline in biodiversity of marine organisms within coastal ecosystems is well known and reported (e.g., Salinger et al., 2020; Behrens et al., 2022; Santana-Falcón and Séférian, 2022; Copedo et al., 2023). Habitat alterations due to climate change have enduring impacts on various invertebrate populations and community resilience, resulting in shifts in ecological structure (Lotze et al., 2006; Subritzky, 2013; Soon and Ransangan, 2019; Montie et al., 2023). Globally, anomalous events of prolonged above-average warm water have increased in frequency and intensity. These prolonged warming events have been termed marine heatwaves (MHWs) (e.g., Houghton et al., 2001; Petes et al., 2007; Smale et al., 2019; Salinger et al., 2020; Copedo et al., 2023; Montie et al., 2023). MHWs can directly affect abalone as well as indirectly through influencing food supply and habitat (Rogers-Bennett et al.,

* Corresponding author. Cawthron Institute, Nelson, 7042, New Zealand.
E-mail address: Joanna.copedo@cawthron.org.nz (J.S. Copedo).

https://doi.org/10.1016/j.marenvres.2025.107090
Received 26 August 2024; Received in revised form 3 March 2025; Accepted 15 March 2025
Available online 16 March 2025

2010). Although temperature is one of the key factors affecting aquatic organisms, other covarying environmental stressors, including increasing sedimentation and increased extreme weather events, also need to be considered (Rogers-Bennett et al., 2010; Nguyen et al., 2021).

Abalone populations are well known to display high morphological variability in growth, whereby the maximum size and growth rate vary both geographically and temporally. These large-scale variations can result in the appearance of slow-growing phenotypes (commonly termed as 'stunted') within the population (Schiel, 1993; Trussell, 1996; Steffani and Branch, 2003; Naylor et al., 2006; Saunders et al., 2009; Subritzky, 2013; Copedo et al., 2024). Slow-growing variants are common in many species of abalone, including *Haliotis rubra* (Saunders et al., 2008) and *Haliotis iris* (McShane et al., 1994), as well as several other molluscan species, such as *Mytilus galloprovincialis* (Hine, 1997), with stunted variants occurring with a smaller maximum size with shorter, wider and higher shells when compared to the fast-growing/- typical growth conspecifics (McShane et al., 1994; Saunders et al., 2009; Van Nguyen et al., 2023). The growth rate of many molluscs responds to a complex relationship between endogenous and exogenous factors. Some of these contributing factors are population density, feed availability, water chemistry, reef topography, hydrodynamics of the microhabitat, pathogen load and immune response (Diggles et al., 2002; Searle et al., 2006; Morash and Alter, 2016; Ren et al., 2019; Saulsbury et al., 2019). For example, a low energy hydrodynamic habitat could result in higher recruitment of larvae in the area versus a higher energy habitat where larvae can drift further, which impacts the population density and food availability (Ragg, 2023). In addition, warming waters and reduced kelp diversity, in association with climate change, have been observed to correlate with slower than normal growth in abalone (Saunders et al., 2009; Rogers-Bennett et al., 2010).

Locally known as pāua, *Haliotis iris* (blackfoot abalone; Gmelin, 1791) is the largest and most abundant of the abalone species endemic to New Zealand (NZ) (Sainsbury, 2010; Gnanalingam et al., 2021). *H. iris* is not only culturally significant but is also an ecosystem engineer, is prized by the recreational fishery, and supports a significant commercial fishing industry (Subritzky, 2013; Gnanalingam et al., 2021; MPI, 2023a; Pāua Industry Council, 2023). Although harvesting is nationally managed using QMAs (quota management areas), *H. iris* is still vulnerable to overfishing, due to a number of factors including its slow growth, aggregation behaviour, reproductive biology, challenges in setting an appropriate minimum legal harvest size based on regional pāua growth rate differences, and changing environmental challenges e.g., habitat disturbance and climate change (Houghton et al., 2001; Gordon and Cook, 2004; Gnanalingam et al., 2021; Van Nguyen et al., 2023).

Slow growing (or stunted) *H. iris* populations, which typically do not reach the minimum legal catch size of 125 mm shell length have been observed in several areas of the NZ coastline (McShane et al., 1994c; Naylor et al., 2006). These populations are typically found in sheltered areas with low food availability and low wave action (Saunders et al., 2009; Laferriere, 2016). The complex interactions of factors influencing growth can lead to additional challenges in the management of *H. iris* populations. Depletion of *H. iris* stocks in the central to southern region of the North Island of NZ (QMA 'PAU2'), in 2023 was reported by customary and recreational fishers. These reports raised resource managers' concerns around the sustainability of these stocks and the impacts of increasing extreme weather patterns, which led to the reduction of the recreation catch limit for pāua collections (MPI, 2023b). Commercially, stakeholders generally report a sustainable commercial fishery. Industry management is formalised by annual operating plans outlining management tools to support the pāua populations. QMAs are divided into micro regions (statistical areas) whereby harvest catch and minimum harvest size are applied at fine scales, taking into consideration the growth rate, length at maturity and habitat type, in order to support and enhance the fishery. Further understanding the cause of differential growth among abalone populations will allow for more targeted management strategies, thereby further supporting the objectives outlined in the plan and ensuring further sustainability (Van Nguyen et al., 2023). Although determining the impacts of environmental change is often complicated by the confounding influence of fishing pressures, understanding the effects of environmental stress on abalone biology is also key for managing populations (Morash and Alter, 2016; Roussel et al., 2020).

The Chatham Islands are located about 800 km off the coast of NZ and comprise of an archipelago of approximately 10 islands, the two largest are the main Chatham Island and Pitt Island. The main Chatham Island supports a large *H. iris* fishery. The minimum legal size of 125 mm has historically created localised areas of low and high fishing effort as a result of slower- and fast-growing populations. In addition to proposing harvest guidelines, the Chatham Island pāua management area committee (PauaMAC4) actively promotes research to identify new management strategies to support population growth (Venter et al., 2022; Van Nguyen et al., 2023). Additionally, the Chatham Islands are biogeographically isolated, and hence experience minimal local anthropogenic influence, but are vulnerable to global climate change, being situated in a warming region with an increasing number of MHW days (Montie et al., 2023). Abalone from the Chatham Islands therefore represent a rare case study opportunity of proactive fishery management in a changing ocean.

A histopathological approach was taken to investigate contributing factors to differential growth between two populations on the main Chatham Island. The populations are exposed to a range of different conditions i.e., physical environment (e.g. wave exposure), and nutrition (e.g. influence of food quality and quantity), which are further described in Venter et al. (2022), Van Nguyen et al. (2023) and Copedo et al. (2024). Collections of *H. iris* at both sites were extended over three years to provide an indication of variability over time, particularly in response to summer marine heatwaves of varying intensity. This study ensured repeated population sampling aimed at exploring the relationship between tissue health, pathogen burden, perceived growth performance and potential vulnerability during summer heatwave events. Results and inferences strive to inform directions for further work and management options for *H. iris* exposed to different environmental conditions, nutrient deficiencies, and pathological findings.

2. Methods

2.1. Environmental monitoring: Estimation of SST for Chatham Islands

While the geographic isolation of the sample locations made *in situ* environmental monitoring impractical, the principal driving variable of sea surface temperature (SST) was determined remotely through satellite. SST data were acquired using daily satellite information from Group for High Resolution Sea Surface Temperature (GHRSST) MUR L4 product (Chin et al., 2017) and the following data portal:

https://oceanlab3.rsmas.miami.edu/erddap/griddap/jplMURSST41.html. Due to the coarse resolution of the satellite, SST was estimated about 4 km away (latitude 43.99°S, longitude 176.34°W) from both sampling sites (sites 1 and 2) although considered as representative. Sea surface temperature anomaly data was sourced from NOAA Coral Reef Watch (https://coralreefwatch.noaa.gov) using a 1985–1990 plus 1993 climatological baseline period to calculate anomalies (Liu et al., 2014). The month of December was selected for visual representation of the SST anomalies for the New Zealand and Chatham Islands region for the years 2020, 2021, 2022 and 2023 for comparison. Whereby zero is the baseline average and SST anomalies are the degrees Celsius above or below the average.

2.2. Sampling location and animal collection

Two sites were selected around the Chatham Islands, New Zealand, based on performance differences of resident abalone (historic data and personal communications: Pāua Industry Council Ltd) as well as initial

sampling and screening assessment (Venter et al., 2022; Van Nguyen et al., 2023). Site 1: Ascots (44°00′56″ S 176°23′12″ W) supports a population of *H. iris* identified as faster-growing, while site 2: Owenga (44°01′28″ S 176°21′56″ W) supports a population of slow-growing *H. iris* (Venter et al., 2022; Van Nguyen et al., 2023).

Ten adult (125.5 mm ± 6.8 mm shell length) and 10 sub-adult (92 mm ± 10.4 mm) *H. iris* were randomly collected by a research diver using SCUBA from each of the two sites at each designated timepoint (Table 1). Adults were classified as those above 110 mm and sub-adults below 110 mm at both sites (Copedo et al., 2024). Sample preparation during the first collection event (March 2020) was completed on site on the day of collection (Copedo et al., 2024). For subsequent samples, individual *H. iris* were transported alive (6 °C humid air) to Auckland University of Technology (AUT), Auckland, New Zealand. The animals collected were weighed to the nearest 0.01 g, followed by measurements of shell length, width, and height (nearest 0.01 mm) before histological preparation. Additionally, the sex of each individual animal was recorded if identifiable (based on the colour of the gonad which was white/cream in males and green in females) and confirmed using histological techniques. Unidentifiable sexes were only detected in the sub-adults (13 of the 114). The sex ratio was determined as the proportion of males among the sex-verified individuals.

2.3. Histopathology

Abalone were shucked using a blunt shucking blade to detach soft tissues from the shell. The viscera was transversally sectioned in three positions, as per Copedo et al. (2024) and Poore (1973) to acquire three, 5 mm histology cuts to maximise chances of sectioning crop/stomach, digestive gland, gill, gonad, left and right kidney (determined histologically by organ architecture (Handlinger, 2022)), adductor muscle and heart (Fig. 1).

The sections were placed into histological cassettes and immediately fixed in 4 % formalin in 1 μm filtered seawater for 48 h. Following fixation, the samples were transferred to 70 % ethanol. Samples were sectioned and stained with haematoxylin and eosin (H&E) at either the histopathology department of Medlab Central (Palmerston North, NZ), or Awanui Veterinary (Formerly: Gribbles, Christchurch, NZ). Additional stains, such as Ziehl-Neelsen (ZN) for haplosporidians (Diggles et al., 2002), Periodic acid/Schiff (PAS) and Periodic acid/Schiff- Diastase (PAS-D) for polysaccharides were also used on selected samples (Howard, 2004; Carella et al., 2018). An additional small section of right kidney tissue was also collected and stored in 100 % ethanol for further molecular analysis.

2.3.1. General tissue alterations

Histology preparations were observed by light microscopy using an Olympus BX35 at magnifications of ×40 to x1000. Eleven tissue-specific alterations were scored as presence/absence or semi-quantitatively, as described below, in relation to site and timepoint. Semi-quantitative assessment included the following: ceroid material deposition (brown pigmented oxidised lipid material) in connective tissue of right kidney, digestive gland and surrounding intestinal tract, as well as kidney stones (Copedo et al., 2024), haemocytosis, digestive gland atrophy, organ/-tissue inflammation, gill epithelial atrophy or cilia loss (Perez-Cebrecos et al., 2022), gill protein level (Hooper et al., 2014), as described previously by Knowles et al. (2014), whereby 0: Absent, 1: Mild or minor changes to the tissue structure, 2: Moderate, ½ of the organ disrupted, 3: High, up to ¾ of the tissue disrupted and 4. Severe, marked disruption and majority of tissue structure affected. The macroalgal quality within the stomach cavity was scored semi-quantitatively on a scale of 1–5 whereby 1 was 100 % fresh with larger pieces of algae and 5 was 100 % old, whereby algae were degraded/digested to mostly fine particles, as previously described by Copedo et al. (2024).

2.3.2. Reproductive staging and egg viability

Female and male gonad development was categorised and graded using a generalised scheme adapted from Vélez-Arellano et al. (2015) and Shin et al. (2020), as described in Table 2:

The proportion of individuals presenting gonads at each stage of development was plotted for visual representation (Fig. 4). An average maturation score was calculated as the number of individuals at each stage identified as the grade. For each of the females detected, further analysis was done to quantify pre-spawning atresia. Atresic oocytes were determined as those that were degrading and being reabsorbed. Identification included: cytoplasmic discolouration and darker staining giving a necrotic appearance, irregular jigsaw shape, as well as retraction and detachment from the jelly membrane. Three microphotographs were taken of the gonad of each female using cellsens imaging software (Olympus cellsens 3.1 [build 21,199]). The objective of an Olympus BX53 was set at x20, and three images of the gonad were randomly collected. For each image, the number of viable developing or vitellogenic and non-viable (atresic) oocytes were counted and recorded. The method proposed by Beninger (2017) was used to derive a percentage of atresia per individual egg-bearing pāua that had been graded as developing or mature (Late or ripe). Spent females were included for visual representation but not included in the pre-spawning atresia analysis.

2.3.3. Pathogens and parasites

Parasites observed within the *H. iris* were identified histologically were recorded as present/absent. Additionally, ciliates previously identified through histology were freshly observed by dissecting a 10 mm section of live gill tissue and examining it using an Olympus dissecting microscope. The plasmodia of a haplosporidian-like parasite in the right kidney tissue previously described by Diggles et al. (2002) and detected by Copedo et al. (2024) was also initially recorded by presence/absence but was subjected to further analysis and further histological staining, as described in Section 2.3. Upon detection of the plasmodia in the right kidney, the length of 35 plasmodia was measured (longest point) to ± 0.01 μm across three individual abalone (n = 15, n = 10, n = 10). The nuclei of five of the pre-measured plasmodia per individual *H. iris* were counted. Further to the measurements and counts of the plasmodia, individual abalone with plasmodia detected were analysed for parasite intensity. Once visual detection occurred using the x40 objective, a count was initiated followed by counts in an additional 24 randomly selected fields using cellSens™ software (Olympus cellsens Standard 3.1 [build 21199] on an Olympus BX53 compound microscope). The first count on initial detection was also included in the analysis as a result of the focal clustering of larger numbers of the plasmodia in few kidney tubules. Removal of these counts from several individuals resulted in a score of 0. The 25 counts were then averaged to provide a relative intensity score per individual abalone. Six of the corresponding ethanol fixed right kidney samples with a range of plasmodia intensities were selected for targeted molecular identification using PCR and metabarcoding methods see Section 2.3.4.

Table 1
Sampling numbers and time course of *H. iris* sampling for the Chatham Islands. The first timepoint (March 13, 2020) has previously been analysed (Copedo et al., 2024) and is included as a reference for comparison.

	Site 1: Ascots		Site 2: Owenga		Reference
	Adults	Sub-adult	Adults	Sub-adult	
March 13, 2020	10	10	10	10	Copedo et al. (2024)
November 26, 2020	10	10	10	10	
March 04, 2021	10	10	10	10	
April 02, 2021	10	10	10	10	
May 15, 2021	10	10	10	10	
April 07, 2022	10	4	10	10	

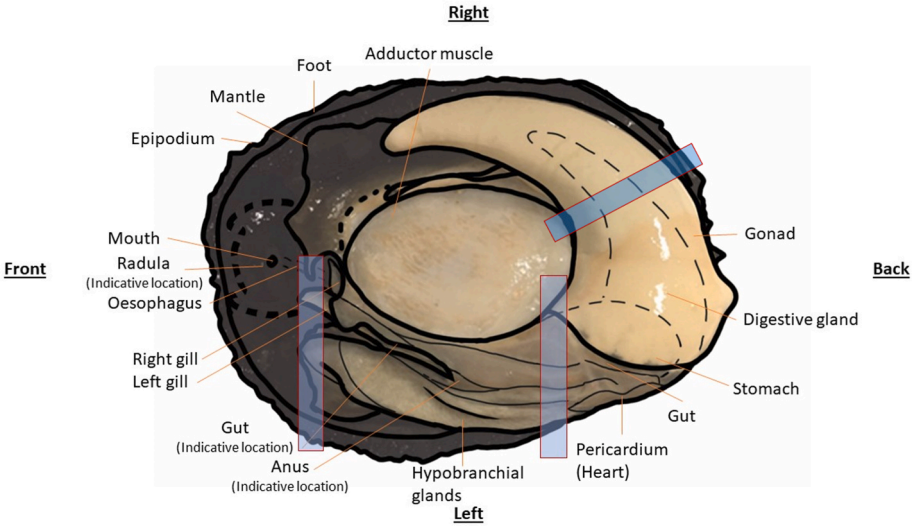

Fig. 1. General anatomical depiction of New Zealand abalone (*Haliotis iris*) by (Copedo et al., 2024). Location of the histology sections, indicated by rectangular windows, were chosen to maximise likelihood of acquiring all tissue types, including gastrointestinal tract, digestive gland, gill, left and right kidney, hypobranchial gland, nervous tissue, muscle and gonad.

Table 2
Generalised reproductive gonad staging descriptions of *Haliotis iris*.

Gonad stage	Grade	Description
Resting	0	Early inactive stage where sex is generally unidentifiable
Early	1	Early inactive with mostly primordial or previtellogenic cells; sex determination is possible
Late	2	Gonad/follicles are developing vitellogenic (formation of yolk protein) oocytes and spermatogonia, the appearance of mature well-developed oocytes and sperm cells. Many primordial/previtellogenic cells observed
Ripe	3	Gonad at full maturity with very few previtellogenic cells in female and mostly large, well developed oval oocytes with a thick jelly membrane and, in males, dense, numerous mature sperm cells
Spawning	1	Loss of mature cells due to the spawning process
Spent	0	Degenerating stage whereby the follicle is observed to have atresic oocytes and/or reabsorption of gametes through the process of phagocytosis
Redeveloping	1	Evidence of recent release of gametes but still has developing previtellogenic and vitellogenic cells

2.3.4. DNA isolation, PCR and metabarcoding sequencing

Molecular analysis was used to corroborate the putative diagnosis of haplosporidian infection, using primers for previously observed *H. iris* haplosporidians (Reece and Stokes, 2003) and generic eDNA primers to detect alternative pathogens. DNA was extracted and purified from approximately 20-25 mg of the ethanol preserved right kidney tissue for each of 6 haplosporidian-like parasite infected *H. iris* individuals using a DNeasy Blood and Tissue kit (Qiagen, Hilden, Germany) according to the manufacturing protocols. As a result of PCR inhibition regularly associated with mollusc native DNA (Adema, 2021), a preliminary PCR was performed on a cascade dilution of 0x, 10x, 100x and 1000x of the DNA extracted using 18S rRNA eukaryotic primers Uni18SF and Uni18SR by (Zhan et al., 2013) to identify the optimal dilution factor required for the samples. Following this first assessment, the 10x dilution was selected and used to perform PCR (Fig. 7a). Two methods of PCR were conducted: a targeted approach using the primers 16S-A/NZAH-R1 and 16S-B/NZAH-F4 following methods from Reece and Stokes (2003), designed for the Haplosporidian/Urosporidium parasite in previous publications and a non-targeted PCR using the 18S rRNA eukaryotic primers Uni18SF and Uni18SR by (Zhan et al., 2013), primarily targeting micro-eukaryotes.

For the targeted method, each PCR reaction included 1 μl of 10 mM of each primer, 10 μl MiFy mix (Bioline, Meridian Bioscience), 2 μl DNA (1/10), 7 μl sterile water. For each PCR run, a negative control (RNA/DNA-free water; Life Technologies), and one positive control (Gblock (DNA fragment), diluted 1/10,000) were carried out, PCR thermocycling was completed on an Eppendorf Mastercycler (nexus gradient) using the following profile: 1 cycle of 94 °C for 4 min, then 35 cycles of 53 °C for NZAH-F4 + 16S-B, or 59 °C for 16S-A + NZAH-R1 for 30 s, 72 °C for 1.5 min and a final extension 72 °C for 5 min (Reece and Stokes, 2003). The size of final PCR product was assessed by electrophoresis.

In the non-targeted approach, each 18S PCR reaction included 1 μl of 10 mM each primer, 25 μl MiFy mix (Bioline, Meridian Bioscience), 3 μl DNA (1/10), 20 μl sterile water, a negative control was carried out in duplicate with the PCR mixture without the target. The total volume of the PCR reactions was 50 μl. The following profile was used: 95 °C for 2 min, 40 cycles of 94 °C for 15 s, 52 °C for 15 s and an extension step at 72 °C for 15 s. The 18S PCR positive samples then went through the clean-up method using the NucleospinGel and PCR Clean-up kit (Macherey-Nagel, Germany), and sent for paired-end sequencing on an Illumina MiSeq platform (Sequench, Nelson, NZ).

2.3.5. Bioinformatics

The FASTQ files, containing the sequence data, were demultiplexed and primers removed using CUTADAPT (version 4.2; Martin (2011)), requiring a minimum overlap of 15 bp and no insertion or deletion. To remove low-quality calls, sequences were truncated on their 3′ end at 215 bp and 190 bp for 16S, and at 225 bp and 216 bp for 18S, for the forward and reverse sequences, respectively. Sequences were subsequently quality filtered and denoised using the default parameters of the DADA2R package (version 1.26 (Callahan et al., 2016);) and merged using a minimum overlap of 10 bp. Potential chimeric sequences were removed using the 'consensus' option of DADA2, where sequences found to be chimeric in a majority of samples are discarded.

Taxonomy was assigned using a combination of approaches and databases to increase taxonomic resolution while maintaining confidence in the assignations. Specifically, 18S data was assigned with the RDP Naïve Bayesian Classifier algorithm (Wang et al., 2007) applied on the SILVA reference database (version 132; Quast et al. (2013)) and with blastn and megablast (Camacho et al., 2009) on the GenBank nucleotide database (Benson et al., 2008) using the default values of the 'blastn_taxo_assignment' function of the biohelper R package (Laroche, 2024). Taxonomic assignments from each approach were then combined using

the taxo_merge function of biohelper, which first normalizes taxonomy using the NCBI curated taxonomic database (Schoch et al., 2020), and, if there is consensus (>50 %) across assigned ranks among the different approaches, uses the highest taxonomic resolution among them. Otherwise, it assigns taxonomy to the last common ancestor among the majority (>50 %) of the approaches.

The top potential parasite amplicon sequence variants (ASVs) were selected for deeper exploration. Their sequences were blasted using Blastn (NCBI, https://blast.ncbi.nlm.nih.gov/Blast.cgi), the top 2 to 3 results within in each of the ASVs were collated and the accession number recorded in a table (Table 6). The relative abundance was then determined for each feature based on the number of hits divided by the total number detected.

2.4. Statistical analyses

Statistical analyses were conducted with the R studio interface Build 375 (RStudio Team, 2021) using R version 4.4.0 (R Core Team, 2024). For the morphometric and sex ratio data the March 13, 2020 reference timepoint as cited in Copedo et al. (2024) was also included in the statistical analysis. The morphometric data were combined for all timepoints and analysed using a general linear model using the car, emmeans (Lenth, 2021), and ordinal package. Additionally, the sex ratio data for each timepoint were combined and only site and life stage were considered using chi squared tests. Histological data were analysed using site and date as explanatory factors. Analysis of the semi-quantitative data was performed using a polynomial ordinal linear regression model using the MASS package (Venables and Ripley, 2002). Binomial general linear models were performed on prevalance data MCMCglmm package (Hadfield, 2010). A p value < 0.05 was considered statistically significant. Additionally, for the semi-quantitative data three statistical models were created e.g. 1) site*sample date, 2) site*sample date + life stage (adult vs sub-adult), and 3) site + sample date, the model with the lowest AIC was selected as the model used in the analysis. Gonad scoring was performed using a generalised linear model followed by ANOVA with a type two sums sq.

3. Results

3.1. Temperature

Temperature data from the GHRSST approximately 4 km from site 1 and site 2 indicated temperature offshore to be maximum 17.0 °C and minimum 10.6 °C, during the sampling period between March 2020 and April 2022. However, during the summer 2018 and 2019 SSTs reached 18.2 °C and 17.6 °C respectively. Sea surface temperature (SST) anomaly data indicated regular occurrences above the 1985–1990 plus 1993 baseline temperature, indicating frequent marine heatwave events (Fig. 2).

Based on the timeseries data in Fig. 2 the average anomaly data for December was selected for visual representation for 2020, 2021, 2022 and 2023 (Fig. 3). December 2021 visually appears to be the warmest of the four time periods based on the SST anomaly gradient.

3.2. Morphometric parameters

The morphometric data indicated a significant difference in the whole animal wet weight between site 1 (Ascots) and 2 (Owenga) (Site x Life stage: $\chi^2_{(1)} = 31.4$, $p = < 0.001$), with adults at site 1 being heavier than those at site 2 ($t = 8.2$, $p = < 0.001$). Interactions were found between site and life stage for shell length measures (Site x Life stage: $\chi^2_{(1)} = 11.9$, $p = < 0.001$), whereby the sub-adults at site 2 were recorded to be slightly longer than those at site 1 ($t = 2.2$, $p = 0.03$). There was no difference in shell width or shell height between *H. iris* at site 1 and site 2 (Site: $\chi^2_{(1)} = 0.1$, $p = 0.78$ and Site: $\chi^2_{(1)} = 0.09$, $p = 0.75$, respectively) (Table 3). Therefore, there was no differences in the L:H ratio between the 2 sites (Site: $\chi^2_{(1)} = 1.08$, $p = 0.3$). In terms of the sex ratio, the combined adult (n = 60) and sub-adult (n = 54) data for site 1 indicated a weak significance difference with sex deviating from the 1:1 ratio towards a female dominated population ($\chi^2_{(1)} = 3.7, p = 0.054$) whereas site 2 (adult (n = 60) and sub-adult (n = 60)) was not significantly different from the 1:1 sex ratio ($\chi^2_{(1)} = 2.3, p = 0.13$). However, when considering the adults only for both populations there appeared to be significant deviations whereby site 1 was female dominated and site 2 male dominated ($\chi^2_{(1)} = 5.4$, $p = 0.02$ and $\chi^2_{(1)} = 8.3$, $p = 0.004$, respectively) (Table 3).

3.3. Tissue alterations

The population prevalence for eight of the indices, along with additional semi-quantitative scores is recorded in Table 4. No significant deleterious alterations were detected in the soft tissues. There were significant interactions between the two sites and the collection dates in some tissue conditions (Table 4).

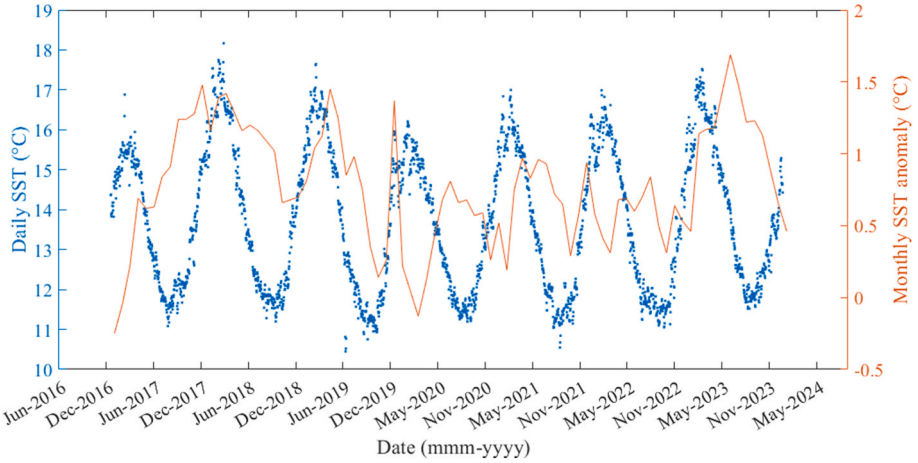

Fig. 2. Course daily sea surface temperature (SST) (Left axis; blue dots) from a single location approximately 4 km from Site 1 (Ascots) and Site 2 (Owenga Harbour) (latitude 43.99°S, longitude 176.34°W). Data source: (JPL, DAAC, 2015). Monthly SST anomaly timeseries from December 2016 to December 2023 (Right axis; orange line). The SST anomaly timeseries shows degrees above the climatological baseline covering the 1985–1990 plus 1993 period (Liu et al., 2014) and is sourced from NOAA Coral Reef Watch (https://coralreefwatch.noaa.gov). (For interpretation of the references to colour in this figure legend, the reader is referred to the Web version of this article.)

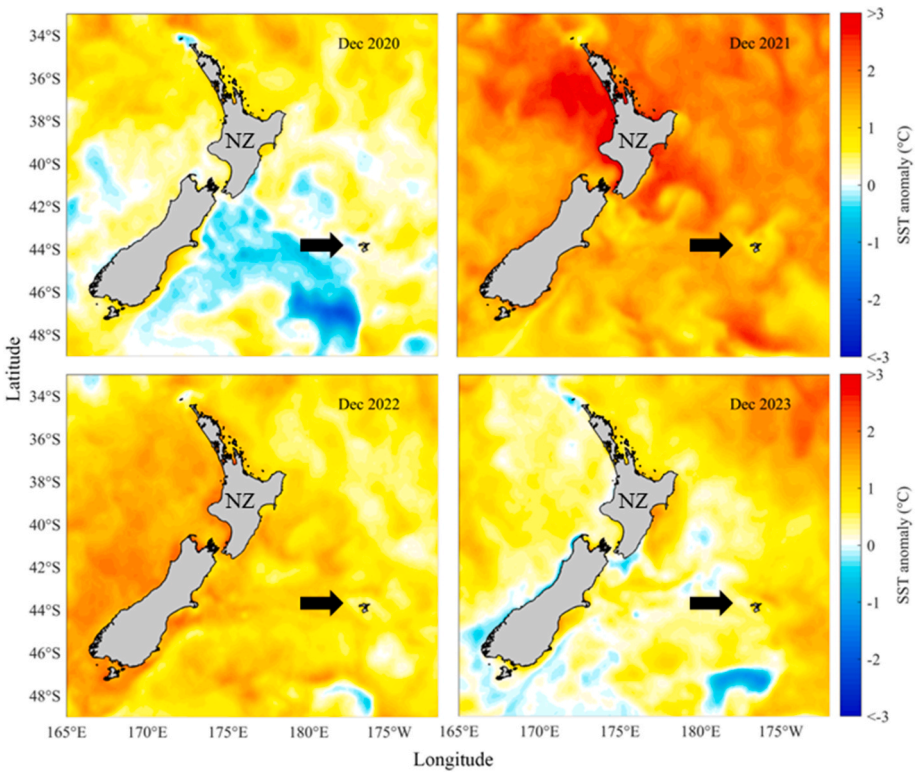

Fig. 3. Visual representation of the average sea surface temperature (SST) anomaly data for the month of December for the years 2020, 2021, 2022 and 2023 around New Zealand (NZ) and the Chatham Islands (arrow). SST anomaly data sourced from NOAA Coral Reef Watch (https://coralreefwatch.noaa.gov) (Liu et al., 2014).

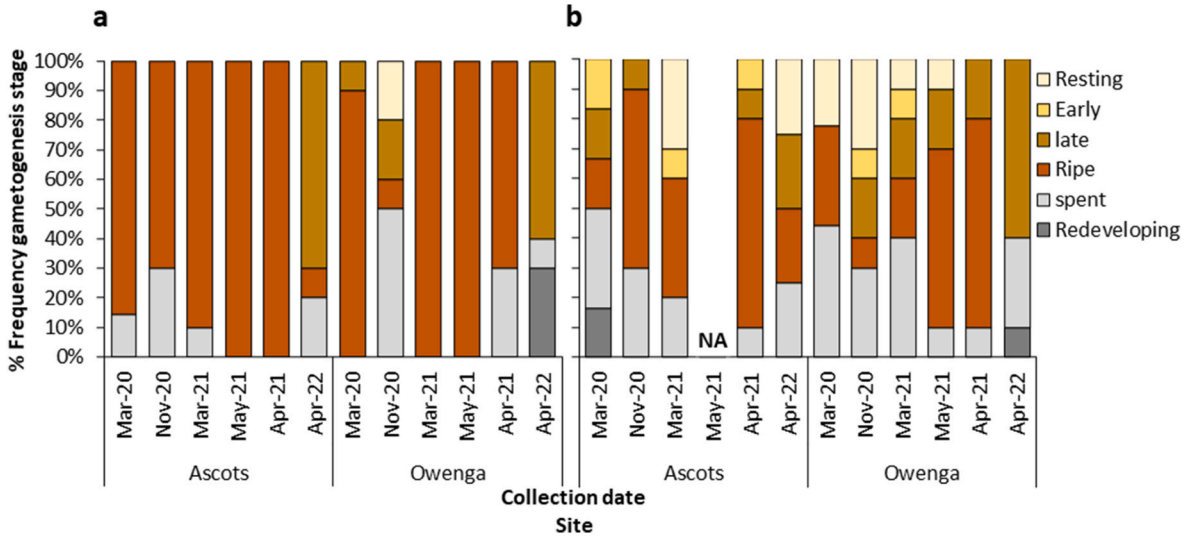

Fig. 4. Frequency of reproductive staging of *H. iris* from 2 sites (Site 1: Ascots and Site 2: Owenga) on the Chatham Islands over multiple timepoints between March 2020 and April 2021 for a) adult abalone and b) sub-adults.

Population prevalences and scores varied between the two locations and sampling timepoints for example elevated ceroid accumulation around the right kidney, digestive gland and sub epithelium of the gastrointestinal tract was detected (Tables 4 and 5). While there was a interaction of location and sample date with the presence of older food detected within the crop/stomach region, no differences were seen between life stages (Tables 4 and 5). For the prevalence of presence of spaces in the interstitial tissue of the digestive gland and kidney stone presence there was no interaction between location and sample date. Differences were also detected in the prevalence of kidney stones, with prevalence regularly above 40 % at site 2 and above 20 % at site 1 while prevalence in the sub-adults was between 0 and 40 % (Tables 4 and 5).

3.4. Reproductive status and atresia

The gonad tissue from most of the adult *H. iris* were observed to be in the ripe stage, with large mature oocytes. The adults at Ascots appeared to be in the ripe stage from November 2020 to May 2021, while adults at Owenga were developing in November 2020 and ripe from March through to May 2021. This resulted in a significant interaction in site and date for the average gonad scoring (Location* sample date: $\chi^2_{(5)} = 11.64$, $p = 0.04$). The sub-adults were observed to spent and early

Table 3
Morphometric and sex ratio data for the adults (n = 60) and sub-adults (n = 54) at site 1 (Ascots) and the adults (n = 60) and sub-adults (n = 60) at site 2 (Owenga Harbour). Data are reported as mean ± standard deviations. The L:H ratio is the length to height ratio and sex ratio is M:F or male to female. Letters indicate statistical differences between site and life stages ($p < 0.05$). For the sex ratio the asterisk (*) indicates significantly different values when compared with a typical 1:1 sex ratio; $p \leq 0.05$ and two asterisks (**) $p \leq 0.001$.

		Weight (g)	Length (mm)	Width (mm)	Height (mm)	L: H ratio	Sex ratio M:F
Site 1. Ascots	Adult	390.7 ± 59.2 a	127.0 ± 7.2 c	88.4 ± 10.8	36.7 ± 8.7	3.7 ± 1.2	0.54 *
	Sub-adult	117.4 ± 57.1 c	87.7 ± 13.5 b	67.0 ± 9.7	23.1 ± 5.1	3.9 ± 0.6	0.95
Site 2. Owenga	Adult	320.6 ± 39.3 b	123.6 ± 6.6 c	91.7 ± 4.9	34.9 ± 6.7	4.3 ± 5.1	2.22 **
	Sub-adult	118.3 ± 28.8 c	92.2 ± 6.8 a	71.1 ± 12.9	24.1 ± 6.3	4.0 ± 0.9	0.79

Table 4
Data for 14 general pathological findings and tissue alterations are presented, including a semi quantitative food score, ciliate (*Scyphidia*-like) prevalence, ciliate intensity (int), gill alterations (e.g., epithelial atrophy or cilia loss), gill protein score (Gill P), haemocytosis (He), ceroid prevalence, ceroid score of the: right kidney (CK), digestive gland (CDG) and sub epithelial layer of the gastrointestinal tract (CSG), detachment of digestive gland tubule from basement membrane (DG gaping), interstitial space between the digestive tubules (DG IS), kidney stones (KS) and haplosporidian-like parasite (Hap) (Copedo et al., 2024), % percent prevalence, * only 1 sample, NR: Not recorded/no samples provided.

Life stage	Site	Collection date	Food score	Ciliate (%)	Ciliate int	Gill alt (%)	Gill P	He (%)	Ceroid (%)	CK	CDG	CSG	DG gaping (%)	DG IS (%)	KS (%)	Hap (%)
Adults	Site 1: Ascots	Mar-20	1.4	100	2.3	0	0.6	0	100	1.0	2.0	1.0	13	20	20	20
		Nov-20	2.8	100	1.4	0	2.9	0	100	0.1	1.6	1.6	89	0	90	20
		Mar-21	2.8	100	1.4	0	1.8	0	100	1.0	1.3	0.4	100	0	50	10
		Apr-21	2.8	100	2.3	0	2.2	0	100	0.5	1.8	1.1	100	0	25	0
		May-21	2.6	100	1.6	0	1.5	0	100	0.8	2.0	1.4	44	0	44	78
		Apr-22	2.9	100	1.8	0	3.0	0	100	1.0	1.0	2.0	0	0	40	20
	Site 2: Owenga	Mar-20	4.9	100	1.8	0	0.7	0	100	3.0	3.0	3.0	100	0	80	60
		Nov-20	3.1	100	1.9	0	1.8	0	100	0.9	2.3	3.0	67	0	89	50
		Mar-21	3.5	100	1.6	0	2.2	0	100	1.5	2.0	2.6	100	20	70	60
		Apr-21	3.7	100	2.2	0	2.6	0	100	2.0	2.1	2.9	88	0	100*	100*
		May-21	3.9	100	1.3	0	1.9	0	100	1.0	2.3	2.9	80	0	71	75
		Apr-22	3.5	100	1.3	0	2.3	0	100	1.8	2.1	2.9	13	0	40	50
Sub-adult	Site 1: Ascots	Mar-20	1.7	100	2.2	0	0.0	0	100	1.0	1.9	1.0	50	0	0	20
		Nov-20	3.1	100	1.5	0	1.7	0	100	0.0	2.1	1.1	40	10	20	50
		Mar-21	2.9	100	1.0	0	1.4	0	100	0.2	1.0	0.0	100	0	10	0
		Apr-21	2.7	100	2.5	0	2.2	0	100	0.0	1.5	0.0	100	0	0	10
		May-21	NR	NR	NR	NR	NR	NR	NR	NR	NR	NR	NR	NR	NR	NR
		Apr-22	3.5	100	2.3	0	3.3	0	100	0.0	1.0	1.0	0	0	0	0
	Site 2: Owenga	Mar-20	4.9	100	2.0	0	1.1	0	100	1.4	2.1	1.4	70	0	20	60
		Nov-20	3.8	100	1.9	0	1.1	0	100	0.0	2.3	2.0	100	20	40	40
		Mar-21	3.3	100	1.3	0	1.9	0	100	0.4	1.6	1.3	90	0	10	70
		Apr-21	4.1	100	1.6	0	2.0	0	100	0.8	1.8	2.2	100	0	0	67
		May-21	3.4	100	1.1	0	2.2	0	100	0.2	1.7	1.2	70	0	0	50
		Apr-22	3.9	100	1.2	0	2.7	0	100	1.5	1.4	2.3	0	0	30	40

developing gonad which also resulted in a difference between life stages ($\chi^2_{(1)} = 26.99$, $p = <0.001$) (Fig. 4).

Atresic oocytes were detected through histological analysis (Fig. 5). The number of atresic oocytes counted in the female adults of *H. iris* was of interest and percentage of affected oocytes was relatively high. There were significant interactions in site and date for the average of the pre-spawning atresia ($F_{(4, 179)} = 4.22$, $p = 0.0027$) and no differences between life stages ($F_{(1, 179)} = 0.4$, $p = 0.53$). The percentage of atresic oocytes was highest at site 1 (Ascots) in adults sampled in November 2020 (74 %) and in the sub-adults in March 2021 (85 %) (Table 6).

3.5. Pathogens and parasites

3.5.1. Histological assessment

Two parasite types were observed in association with *H. iris*. *Scyphidia*-like ciliates (Diggles and Oliver, 2005) and a haplosporidian-like parasite. *Scyphidia*-like ciliates were observed at 100 % prevalence in both populations at each time point (Table 4) and were easily identifiable under a dissecting microscope (Fig. 6a and b). There was a significant interaction in the presence of the haplosporidian-like parasite between site and collection date (Tables 4 and 5). Differences between the collection dates in 2021 were apparent at site 1 for March/April and May ($p = 0.03$ and $p = 0.034$, respectively) (Table 4).

Multinucleate plasmodia of the haplosporidian-like parasite were observed only in the right kidney tissue of several individual pāua. Plasmodia showed similarities to the parasite observed in the right kidney by Diggles et al. (2002) but not seen in the other tissues observed by Diggles et al. (2002) and identified by Reece and Stokes (2003). The average plasmodia length was 14 μm and ranged from 4.91 μm to 22.37 μm, width from 5.39 μm to 9.28 μm (n = 35) and each plasmodium was observed to have between 5 and 8 nuclei (n = 15). The relative intensity (average number) of the plasmodia within the right kidney of *H. iris* were as follows: during March, April, and May adults at site 1: 2.32 (n = 1), 0 (n = 0), 1.16 ± 1.19 (n = 7) and site 2: 1.1 ± 1.1 (n = 5), 5.8 (n = 1), and 2.85 ± 2.1 (n = 6), respectively. For Sub-adults at site 1: 0, 0.08 (n = 1), and 0 and sub-adults at site 2: 1.76 ± 1.25 (n = 4), 1.03 ± 0.5 (n = 4), 1.31 ± 1.2 (n = 5), respectively. No differences were observed between date and site ($f_{(28, 2)} = 0.63$, $p = 0.54$) and site and life stage ($f_{(30, 2)} = 0.01$, $p = 0.91$). Plasmodia were detected using ZN, PAS and PAS-D stains with H&E being the most effective stain for detection overall (Fig. 6 c, d, e, f). In contrast to Diggles et al. (2002) ZN staining indicated that the plasmodia were not acid-fast. The PAS and PAS-D

Table 5
Statistical analysis of the pathological findings and general tissue alterations observed through histology in Table 4. The lines in bold indicate statistically significant values $p < 0.05$.

Scoring method	Alteration	Statistical method	χ2	df	*p* value
Prevalence	Ciliates	Location * sample date	0	5	1
		Life stage	0	5	>0.05
	Gill alterations	Location * sample date	0	5	1
		Life stage	0	5	>0.05
	Haemocytosis	Location * sample date	0	5	1
		Life stage	0	5	>0.05
	Ceroid	Location * sample date	0	5	1
		Life stage	0	5	>0.05
	DG gaping	Location * sample date	0	5	1
		Life stage	0	5	>0.05
	DG spacing	Location * sample date	3.06	5	0.69
		Life stage	**6.5**	**5**	**0.01**
	Kidney stones	Location*sample date	5.02	5	0.41
		Location	**52.09**	**1**	**0.001**
		Life stage	**52.09**	**1**	**0.001**
	Haplo-like parasite	**Location * sample date**	**16.85**	**5**	**0.005**
Semi-quantitative	Food score	**Location * sample date**	**84.67**	**5**	**0.001**
		Life stage	2.38	1	0.12
	Ciliate intensity	**Location * sample date**	**17.86**	**5**	**0.003**
		Life stage	1.37	1	0.24
	gill protein score	**Location * sample date**	**20.05**	**5**	**0.001**
		Life stage	2.31	1	0.13
	Ceroid kidney	**Location * sample date**	**20.75**	**5**	**0.001**
		Life stage	**57.26**	**1**	**0.001**
	Ceroid DG	**Location * sample date**	**12.59**	**5**	**0.028**
		Life stage	**18.78**	**1**	**0.001**
	Ceroid SG	**Location * sample date**	**26.52**	**5**	**0.001**
		Life stage	**100.81**	**1**	**0.001**

Table 6
Average percent of atresic (non-viable) oocytes in females that were graded as spent, ripe or late developing. NR = not recorded, empty spaces = no samples available. Atresia in ripe and late development was considered as pre-spawning atresia.

		Ascots						Owenga					
		Mar-20	Nov-20	Mar-21	Apr-21	May-21	Apr-22	Mar-20	Nov-20	Mar-21	Apr-21	May-21	Apr-22
Adults	**Spent**	90	89	98			95		100		96		80
	Ripe	39	74	55	65	30	47	59		21	49	49	
	Late						59						
Sub-adults	**Spent**	92	96	100	91	NR	100	93	100	98	100	100	93
	Ripe			85	61	NR	38	19		47	49	16	
	Late	25				NR					68	12	

indicated presence of glycogen-like material within the plasmodia bodies. Overall, right kidney tissue appeared to be in good condition and no haemocyte proliferation was detected.

3.5.2. *Molecular identification of parasites*

Two molecular approaches were performed to further identify the haplosporidian-like cells: a PCR targeting the SSU rRNA gene sequence of the haplosporidian-like parasite from NZ *Haliotis iris* (Reece and Stokes, 2003) and metabarcoding.

The PCR analysis performed on the right kidney tissue shows negative results for the haplosporidian-like parasite (Diggles et al., 2002; Reece and Stokes, 2003) except for the positive control (Gblock, Fig. 7), suggesting the observation of a different/new parasite in this study.

A total of 65,431 reads were obtained from the sequenced data. After quality filtering, denoising, paired-end merging and removal of potential chimeric sequences, a total of 100 ASVs and 45,946 reads remained, with a mean of 15,315 reads/sample.

The three main groups detected based on the last common ancestor were Apicomplexa, Sessilida and Haptoria (Table 7). No hits were detected for the previously identified Urosporidium/haplosporidian-like parasite.

4. Discussion

The histological information presented in the current study adds critical seasonal and inter-year dimensions to an initial investigation by Copedo et al. (2024) and provides further information on the site-specific differences between two *Haliotis iris* populations from the main Chatham Island. Marked differences were noted in the *H. iris* tissues between the two sites; however, these differentials varied in significance over time. For example, elevation of ciliate numbers occurred in March 2020 and April 2021 when compared to November 2020 and March 2021 indicating potential seasonal and annual variations. More consistently, tissue condition observations made during the March 2021 collection support those reported by Copedo et al. (2024) in similar-sized individuals sampled in the same month. The increased temporal resolution in the present study confers greater confidence in the detection of pathological findings and tissue alterations including ceroid accumulation, kidney stones, ciliates, and haplosporidian-like plasmodia being associated with slower growth. These combined observations emphasised the health and performance differences between the sites. Food integrity, as an indicator of quality, in the gastrointestinal tract was similar between both populations post-transport to the laboratory. However, based on site characterisations *H. iris* from Ascots had more available algae than Owenga. Although, site differences can only

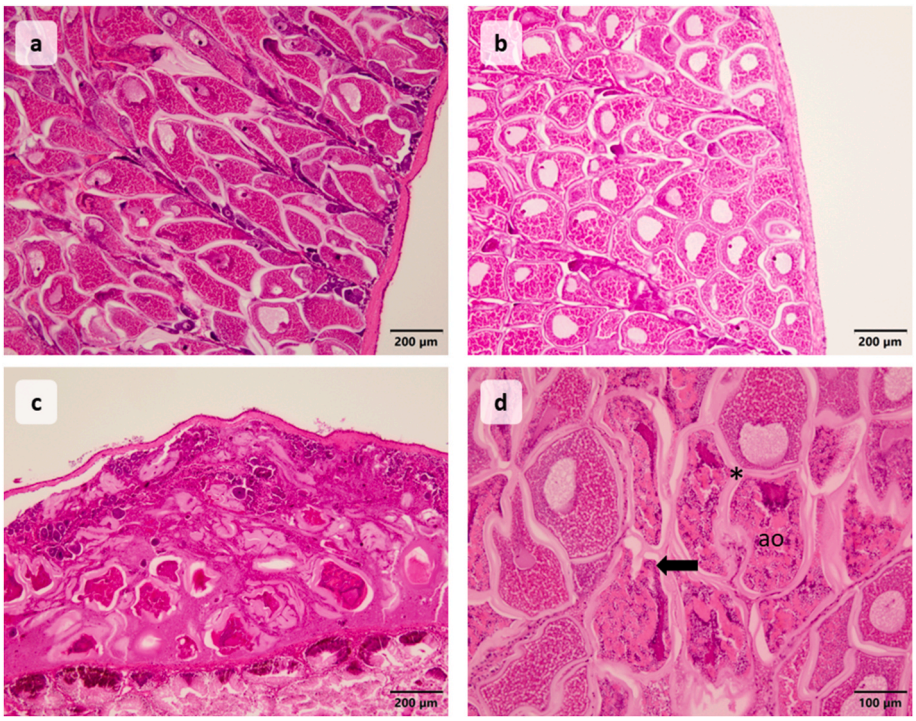

Fig. 5. Representative images of the reproductive staging of female *H. iris* showing a) late-stage gonad development of oocytes, b) ripe stage gonad with mature oocytes, c) spent stage with degrading/atresia oocytes and atresic debris, and d) atresic oocytes (ao) of a ripe stage female indicating potential pre-spawning atresia, jelly membrane of the oocytes (*) and atresic oocyte showing detachment from the membrane (arrow).

be tentatively inferred as availability, diversity and quality of algal species may change over time. *H. iris* from the Owenga site also had increased prevalences of kidney stones, haplosporidian-like parasites in the gut, and elevated ceroid. In addition, this population showed evidence of spawning events and a lower proportion of atresic oocytes when compared with the second site.

4.1. Nutritional stress and an ageing population

Although proportionally wider shells of the slower growing site (site 2, Owenga) were apparent within this study, lengths were similar between the two sites providing an opportunity for 'same size' comparison. It is likely that depleted nutrition contributes substantially to the slow growth due to dietary limitations, as mentioned previously by Bayne (2004), Venter et al. (2022), Van Nguyen et al. (2023) and Copedo et al. (2024). This is supported by Van Nguyen et al. (2023) who found that slower growing *H. iris* from the Chatham Islands, including Owenga, had lower levels of several key organic acids (including some essential fatty and amino acids) circulating in the haemolymph. However, this influence is closely followed in importance by physiological alterations from external and internal stressors (Bayne, 2004). For example, increased sedimentation also impacts nutrient absorption and respiration, which can affect tissue and shell growth (Poore, 1973; Schiel et al., 2006; Saunders et al., 2009; Laferriere, 2016). Additionally, increased population density has been observed to correlate with slower growth and the degree of reproductive development in *H. laevigata* (McAvaney et al., 2004).

Based on the results from Copedo et al. (2024) and A. C. Alfaro (unpublished observations), it appears that algae at site 1 are more abundant, palatable, and easier to digest, with consequently higher consumption. Access to a diverse range of macroalgal species is also known to improve abalone growth (Stuart and Brown, 1994; Mai et al., 1995; Viera et al., 2011). It should, however, be noted that the algal architecture within the stomach/crop region was decayed in samples from both sites post 24–48-h transport, which is consistent with digestion time (Day and Cook, 1995; Britz et al., 1996). It is therefore likely that reduced nutritional quality and quantity of food available (reduced energy availability) to the slower-growing population is limiting growth, while exacerbating other tissue conditions such as ceroid-lipofuscin accumulation. The inferences based on gut content are therefore tentative and would benefit from further *in situ* assessments.

Ceroid and lipofuscin both present as pigmented brown to yellow waxy aggregates and both are by-products of oxidative stress and typically termed as 'ceroid-lipofuscin' due to the similarities (Carella et al., 2015; Miller and Zachary, 2017; Webb and Duncan, 2019; Copedo et al., 2024). Lipofuscin is typically associated with age as a 'wear and tear' pigment in vertebrates where the yellow/brown pigments accumulate as cellular debris, from the lysosomes, in the cytoplasm as part of a normal cellular process. Although similar to lipofuscin, ceroid pigments are considered to be associated with pathological conditions (Dolman and MacLeod, 1981; Zaroogian and Yevich, 1993; Seehafer and Pearce, 2006; Jung et al., 2007b; Miller and Zachary, 2017). Lipofuscin and ceroid can also increase accumulation of lipid peroxidation as a result of their ability to facilitate their own production (Jung et al., 2007a). The lysosomes within the cell may not be able to digest all of the pigment, resulting in the accumulation outside of the cell (Dolman and MacLeod, 1981). The build-up of both lipofuscin and ceroid pigments impairs tissue function and can correlate with impacted growth (Hole et al., 1995). As a result of the similarities between ceroid and lipofuscin and the difficulty of separating the two, the term 'ceroid' will be used generically henceforth.

Incidence of elevated ceroid material within the interstitial tissues of the *H. iris*, was observed to be higher in the adults at the slower growing site (site 2, Owenga) based on the statistical interaction, reflecting a pattern previously observed by Copedo et al. (2024). The increased level of ceroid in the slower-growing population indicates a potential cumulative tissue maintenance cost (Terman and Brunk, 1998). The increase in ceroid, whether from poor nutrition, potential thermal stress from heatwaves or self-driven production is also likely to impact growth by reallocating energy away from growth for general tissue and cellular

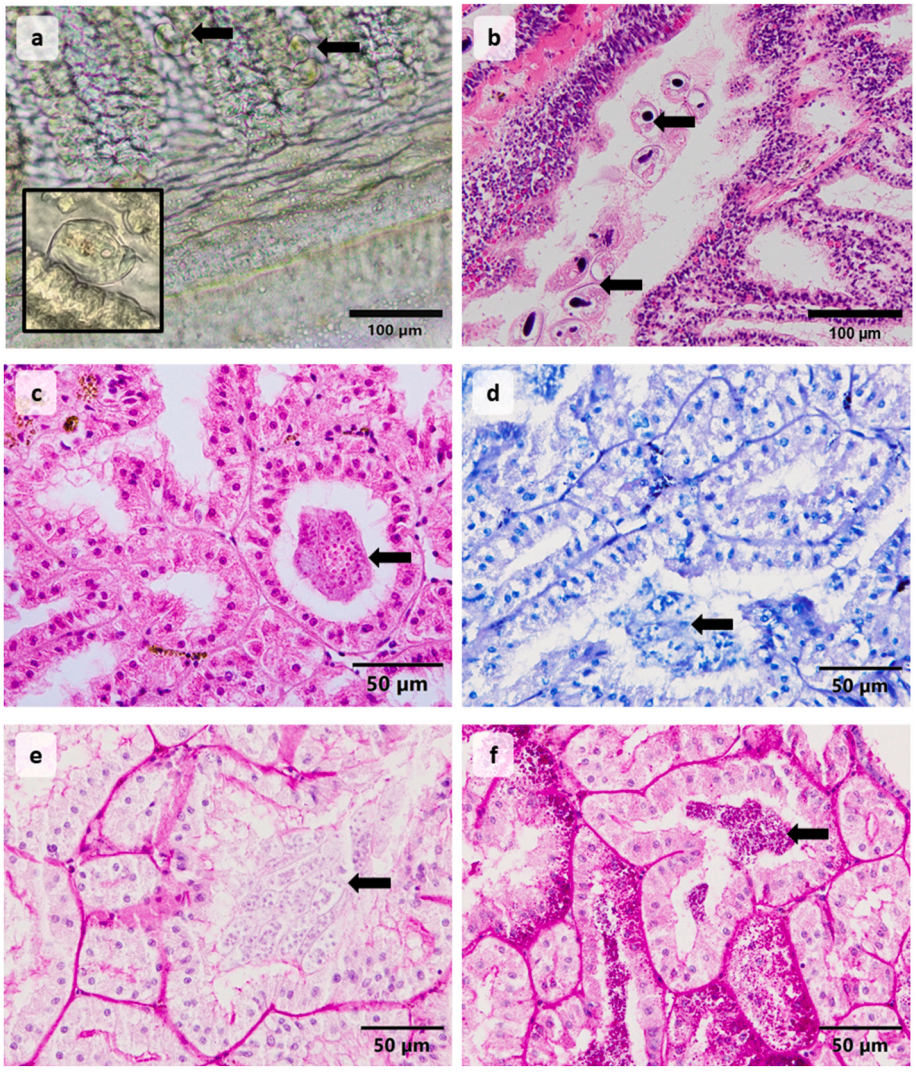

Fig. 6. Photomicrographs of the parasites observed in *H. iris* samples a) gross observation of the ciliates attached to the gills (arrows) inset: enlargement of ciliate attached to gill filament, b) ciliates observed in histology stained with H & E, c) the haplosporidian-like multinucleate plasmodia (arrow) located in the lumen of the right kidney was observed to have refractive spore-like structure H&E, d) the plasmodia in the lumen of the right kidney stained using ZN, e) PAS-D and f) PAS. Plasmodia are indicated with arrows.

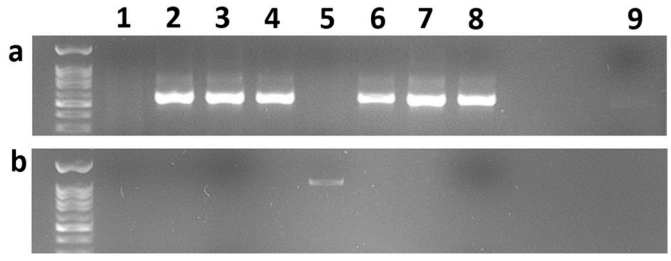

Fig. 7. The PCR Gel results for a) 18s primers using different dilutions of DNA extraction from sample 1: a1) pure, a2) 1/10 concentration, a3) 1/100, a4) 1/1000, and sample 2: a5) pure, a6) 1/10, a7) 1/100, a8) 1/1000, and a9) neg control, b) PCR gel results using NZAH-F4 and NZAH-R1 primers on 1/100 diluted samples b1) sample 1, b2) sample 2, b3) sample 3, b4) sample 4 b5) GBlock, positive control at approximately 1100 base pairs, and b8) neg control, b6, b7, and b9 are empty slots.

maintenance (Portner and Farrell, 2008; Kooijman and Kooijman, 2010; Sokolova et al., 2012; Delorme, 2017; Booth, 2018; Steeves et al., 2018). If the habitat with the slower growing population is warmer, then accumulation of oxidative damage is to be expected, exacerbating the formation of ceroid production (Marigomez et al., 2002; Carella et al., 2015; Shaw et al., 2019; Webb and Duncan, 2019). Finally, if, ceroid production is constant with age and aging is a "progressive loss of physiological integrity", based on the statement by Cohen (2018), then the build-up of ceroid would impair tissue function. Therefore, the slower growing population displays not only a reduced scope for growth because of cellular destabilisation, but also accelerated senescence (age). Although *H. iris* were not aged during this study (e.g., by counting shell growth rings), based on the ceroid differences between the adults and subadults, and the differences between the slower and faster growing populations, as well as the biased sex ratios, and parasite accumulation, there is evidence to suggest that the adults in the slower growing population are older than their faster growing counterparts. However, future investigations should include aging techniques to confirm these findings. Comparisons of physiological age (loose measure of physiological fitness) versus the chronological age (absolute lifespan) (Philipp et al., 2005) between the two populations would definitively confirm the 'slower growing' characterisation. Typically, physiological age and chronological age are positively correlated, however they may not be linear. Furthermore, based on minimum legal catch sizes it is also possible that there is an accumulation of older abalone in the slower

Table 7
Gene sequence results from gene blasting the 18S amplicon sequence variants, of particular interest, of the 3 samples of abalone kidney tissue. The top 2 to 3 closest species were recorded for each of the 3 selected features and the last common ancestor was recorded.

Feature ID	Accession number	Identity	E-Value	Query coverage	Closest species	Last common ancestor	Relative abundance
6f373dbe6cbc5bcd6e50fa56da154f77	MH375329.1	79.86 %	2.00E-72	100 %	*Cryptosporidium* sp.	*Apicomplexa*	0.1 %
	MN493109.1	80.10 %	2.00E-72	100 %	*Theileria* sp.		
0d2c9b0214a245445bae15860cab5201	KP698209.1	95.85 %	0	100 %	*Scyphidia ubiquita*	*Sessilida*	53.7 %
	KP698210.1	93.66 %	4.00E-169	100 %	*MantoScyphidia branchi*		
	ON157280.1	91.55 %	8.00E-156	100 %	*Vorticella* sp.		
6e9fcd2b0c6e21db389e738de2591c7d	KY355505.1	98.86 %	8.00E-175	100 %	Uncultured eukaryote	*Haptoria*	44.9 %
	LN870157.1	96.59 %	2.00E-161	100 %	*Haptoria* sp.		
	OR042381.1	96.58 %	7.00E-161	100 %	*Pseudoamphileptus apomacrostoma*		

growing population which never grow large enough to be removed by fishing activity.

In terms of the sex ratios, the adult populations from the slower-growing site were male dominated when compared to the fast-growing, female dominated, site. This result consistent with the observations of Poore (1973), who suggested that older populations of *H. iris* trended towards male dominance. This is also supported by Lleonart (1992), who observed a male dominated population in *H. laevigata* and attributed it to the females being fished first due to their larger size. However, it is also likely that due to the suboptimal habitat and the energetic investment required to produced oocytes, female mortality could be higher in the slower growing population resulting in a bias towards male survival. Although the slow-growing population histologically appears to have conditions, such as the ceroid and kidney stones, which would influence metabolic maintenance of the tissues, as well as the nutrient deprivation from limited food access and, potential exposure to suboptimal temperatures, they are still reproductively active. Based on these factors (diet, temperature, reproduction), it could be suggested that they have adapted to 'life in the slow lane' (Clarke, 1988; Philipp et al., 2005).

4.2. Site-specific reproductive condition and atresia

The reproductive stages encountered and elevation of oocyte atresia in the adults is of particular interest. Gametogenesis was observed in the November 2020 snapshot, but the ripe gametes appeared to be retained up until May 2021. If these observations represent stasis within the gonad, it becomes unclear when/if spawning occurred in 2021. Additionally, developing gametes were observed in November 2020 at the Owenga site (site 2), which may suggest a previous spawning event (Autumn) and local population differences in each bay. Poore (1973) also observed differences in gametogenesis staging between two sites in New Zealand, whereby at one of the site's spent gonads were very rarely observed whereas all were spent post-spawning at the other site. The results of the present study also support Poore's (1973) original statement regarding the unreliability of making generalisations regarding spawning season when samples are only collected for one year. Although the present study provides only a snapshot of the gametogenesis cycle, the data suggest variability in timing of the spawning season each year. There is variation in spawning magnitude and timing, the broad trends described by Poore (1973) and Wilson and Schiel (1995) suggested development of gametes leading up to the November 2020 sampling could be expected, following the Autumn spawning. This would theoretically be followed by ripening, then spawning associated with the February and March 2021, and potentially April 2021 sample events, depending on localised variability. Few studies on *H. iris* in New Zealand have focused on the histological staging of reproductive development over multiple seasons. This is particularly so with respect to localised populations and changing climate, but such knowledge gaps indicate profitable future directions for research. A further area for investigation would be the assessment of gametogenesis patterns and differential oocyte quality between populations across multiple years to build on the data and provide greater confidence in interpretation.

There is generally high variation in the spawning season of haliotids with some species maintaining condition for months and others such as *H. iris* having discrete spawning seasons (e.g., Webber and Giese, 1969; Poore, 1973; Wilson and Schiel, 1995). Additionally, spawning failure is not uncommon, Poore (1973) and Sainsbury (2010) both reported years where there was no spawning detected, for example 1969 and 1974, respectively. According to Poore (1973), temperature alone could not explain spawning failure in 1969, due to a successful site having a similar temperature profile. Gonad production is an energy demanding process that can impact behaviour and growth rate: during the winter period shell growth slows and correlates with the production of gonad (Poore, 1973), highlighting the value in exploring energy balance as a means to interpret variability in reproductive performance. Furthermore, controlled experiments are required to assess the relationship between reproductive performance, temperature and nutrition.

In addition to the unusual reproductive staging results, there was also an increase in appearance of pre-spawning atresia (oocyte resorption) in the adults. The increase in atresia is potentially indicative of a delayed spawning and a sub-optimal environment (Beninger, 2017; Chérel and Beninger, 2017). The percent of atresic oocytes was observed to be higher in the faster growing population and could potentially support the hypothesis that atresia is removing older oocytes, to favour development of the younger oocytes, rather than over-investing in a single spawning event. Atresia is known to be a reabsorption strategy of energy recycling during adverse conditions, such as thermal stress (Beninger, 2017; Chérel and Beninger, 2017). It has been observed in several mollusc species including, clams, mussels, and oysters (Steele and Mulcahy, 1999; Pérez et al., 2013; Chérel and Beninger, 2017; Copedo et al., 2023). In a previous study (Wilson and Schiel, 1995), resorption of oocytes in *H. iris* was also noted during the lead up to spawning, as well as during recovery post-spawning, indicating removal of mature oocytes. Also, for *H. discus hannai* it was found that oocyte quality improved, in terms of lipid and protein content, after the first spawning and post reabsorption, resulting in more consistent survival of the larvae (Fukazawa et al., 2005).

Although Poore (1973) could not attribute temperature to the spawning failure, temperature does influence the reproductive cycle of many species of *Haliotis* and can potentially alter reproductive phenology (Poore, 1972; Wilson and Schiel, 1995; Kim et al., 2016). It is also known that spawning events occur after a change in temperature and typically occur as water temperature starts to decline (Poore, 1972;

Wilson and Schiel, 1995; Kim et al., 2016). Disruptions associated with ocean warming, e.g. temperature, habitat alteration and food availability, can also impact reproductive condition and therefore spawning (Moss, 1998). The present study therefore highlights the need for ongoing multi-year sampling to build a reliable gametogenesis map for *H. iris* particularly regarding the changing climate. Additionally, further research confirming scope for growth and impact of temperature is required to resolve questions such as, whether the fine-scale genetic variability underpins the site-specific growth patterns, whether there is a greater benefit of being larger or smaller under stress whether temperature will impact spawning cues, and how the occurrence of pathogens further impacts growth and reproduction.

4.3. Pathogens

The detection of 2 groups of ciliates, the first being *Sessilida* and the second *Haptoria* in the metabarcoding analysis was expected as there was a high number attached to the gills of the *H. iris* and 100 % prevalence in both populations. Numerous species of ciliates also live in association with aquatic molluscs (Bower, 2006). Previous studies on *H. iris* have detected ciliates on the gills and determined them to be either *Sphenophyra*-like or *Scyphidia*-like (Diggles et al., 2002; Muznebin et al., 2021; Copedo et al., 2024). The high DNA metabarcoding identity score of the groups indicates that the ciliates detected on the gills are likely to be *Scyphidia* sp.

The detection of the haplosporidian-like plasmodia within the right kidney tissue of adult *H. iris* were initially of concern due to the >50 % population prevalence in the adults of site 2, and >40 % prevalence in the sub adult population of site 2, as well as a similar occurrence associated with a mortality event in juvenile *H. iris* reported by Diggles et al. (2002), Hine et al. (2002) and Reece and Stokes (2003). However, unlike the above studies, within the current study no other plasmodial parasites were observed in other tissues histologically. Based on results of Copedo et al. (2024), the right kidney tissue was targeted within the present study to investigate the parasite and provide more taxonomic information. It was found using targeted and non-targeted (metabarcoding) PCR techniques that the parasite in the right kidney within this study was not the same as previously identified by Diggles et al. (2002) and Reece and Stokes (2003). The current parasite within the *H. iris* was only detected in the right kidney lumen of both life stages (adult and sub-adult) and no immune response or mortalities were associated with it. Furthermore, in contrast to the parasite detected within this study the juveniles in Diggles et al. (2002), Hine et al. (2002) and Reece and Stokes (2003) presented with a plasmodia stage of a novel parasite in most tissue types (e.g. gill and epipodium etc.). Diggles et al. (2002) also reported the haplosporidian-like plasmodia in the right kidney of adult *H. iris* and suggested the low numbers and prevalence could be representative of a natural infection, and thus adults could potentially be asymptomatic carriers. Whereby, the question remained whether the parasite detected within this study is the same species previously described and observed or whether they were a coincidental occurrence. In addition, based on Diggles et al. (2002) study, the parasites were associated with poorer host growth, with results from Reece and Stokes (2003) placing it closer in the phylogenetic tree to *Urosporidium*. Little is known about the haplosporidian-like (*Urosporidium*) parasite found in *H. iris* by Diggles et al. (2002) and Hine et al. (2002) or the host-pathogen interaction particularly in regards to climate change.

The metabarcoding analysis also identified the presence of apicomplexans (*Cryptosporidium* and *Theileria* sp.). *Theileria* sp. and cryptosporidians are protozoan parasites of mammalian species. Cryptosporidians are typically found in cattle faecal matter which can contaminate shellfish, particularly if the waters are polluted by anthropogenic discharge (e.g. livestock faeces during rain events) (Srisuphanunt et al., 2009, 2023). *Cryptosporidium*-like cells have previously been observed adhered to the mucosa layer of the intestine in abalone (Handlinger et al., 2002), so detection is not unexpected in the *H. iris*. Detection, of *Cryptosporidium* in the kidney tubules is likely incidental and represents contamination from the main gut section (Handlinger et al., 2002). However, *Cryptosporidium* is also a member of the apicomplexan group (Rajapandi, 2020), along with Eimeriidae, which causes renal coccidiosis in several molluscan species (Chong, 2022). Due to the low identity value of the Apicomplexa group, the limited genetic data of New Zealand parasites (Thomas et al., 2022), small sample number, and the possibility of low quality DNA or degradation, the haplosporidian-like parasite could not be identified further. Based on the molecular results it is hypothesised that the parasite belongs to the apicomplexan group rather than the ciliate or haplosporidian/Urosporidium group, but further molecular research is required for species specificity. Additional research is required to confirm and validate the parasites detected in the kidney tissue of Chatham Island *H. iris*. Regardless of parasite specificity based on previous pathogen research on emergence and spread, such as *Perkinsus olseni,* a protistan parasite (Muznebin et al., 2021; Lane et al., 2023), the information presented provides a potential early warning of a parasite that may impact the *H. iris* in the future.

4.4. Contributing factors to slow growth and future vulnerabilities

The lack of amino acids observed previously in algal food (Van Nguyen et al., 2023) and the limited and poor algal quality inferred in this study implicates inadequate nutrition as a key influence on slow growth. Although ceroid deposition in the tissues was unlikely to be the initial cause of the slow growth, once it reaches an intensity where it propagates it is likely to have cumulative impacts on the energy budget. Furthermore, both sites showed signs of gametogenesis, presence of kidney stones (right kidney), and parasites which represent additional energetic demands on the *H. iris* because of energy reallocation and immune defence. Due to these additional energetic demands the energy available for growth is likely limited, resulting in slower growth.

The Chatham Islands sit in a marine heatwave hotspot, which regularly experiences anomalous sea surface temperatures and extended MHW days (Montie et al., 2023). Although approximate maximum temperatures during the sampling period remained below 17 °C there were strong sea surface temperatures anomalies observed during this period. In addition, the previous two summers showed temperatures reaching ~18 °C. Elevated temperature can interact and exacerbate the conditions discussed above, and impact the overall metabolic scope, thus further reducing available energy. In a study by Nguyen et al. (2023), it was found that with prolonged periods (weeks) of temperature above 18 °C *H. iris* could not reduce their energy expenditure, resulting in energy demand exceeding supply, leading to a vulnerability to thermal stress during the summer period. However, it is also likely that local adaptation of *H. iris* to cooler temperatures in the Chatham Islands mean that lower thermal tolerance is possible. Furthermore, increasing sea temperatures due to climate change are likely to impact local seaweed abundance and diversity. It is well known that marine heatwaves threaten marine biodiversity resulting in impacts on kelp forests, resulting in compromised future food sources for *H. iris* (Rogers-Bennett and Catton, 2019; Thomsen et al., 2019; Rogers-Bennett et al., 2021; Nguyen et al., 2023). The food supply, temperature, and parasite presence observed within the current study, as well as other research (Morash and Alter, 2016; Venter et al., 2022; Nguyen et al., 2023; Van Nguyen et al., 2023), indicate that *H. iris* populations are likely to be vulnerable to climate change phenomena, notably marine heatwaves. In addition, research by Nguyen et al. (2023) and Aalto et al. (2020) also indicate that the adult life stage is likely the most vulnerable to future environmental stressors.

5. Conclusions

This histological investigation provides key information about the factors contributing to slow/stunted growth in New Zealand abalone.

The following factors were implicated: site, environment, parasites, pathology, reproduction, as well as nutrition as previously described in Copedo et al. (2024), exacerbated by a likely vulnerability to increased temperature. pathological findings observed (e.g. ceroid) were primarily detected in the adult populations which could indicate that growth differentials start to occur once the individuals reach maturity. If ceroid is an indicator of age and production is constant, then even without chronologically aging the shells, its presence supports the anecdotal observations of growth differences. The current study highlights several dynamic parameters following on from the initial March 2020 investigation to further elucidate population differences. Further information on the gametogenesis cycle over multiple years, spawning failure, and recruitment of new juveniles of *H. iris* are critical, not only in a changing climate but also under the additive pressure of fishing. In addition, further monitoring of the gametogenesis cycle will also provide key knowledge in understanding growth phenology and energy allocation. In parallel to the monitoring of growth and reproduction, a means of assessing age across a large size range and quantifying ceroid deposition would also be beneficial in determining the relationship between chronological and physiological age. Finally, pathogens present a potential threat; the parasite observed in the right kidney tissue in wild *H. iris* deserves particular attention, noting that it could also provide a potential early warning of future health problems. Such possibilities could be assessed if there is greater knowledge of host/parasite interactions under the influence of climate change. Further work should include the impact that this parasite may have on the population in the future and the implications for fisheries management.

Improving knowledge on the following: seasonal and annual variation in seaweed diversity, gametogenesis and oocyte quality of the *H. iris* thermal stress, energetic budget, and initial cause of ceroid deposition (e.g. age or stress) would provide beneficial information to support other management strategies already being implemented by fishing industry. These factors and pathological findings, as discussed above, are also likely to increase the vulnerability with increasing pressure during summer heatwaves. Due to changing climate, increasing abnormal weather patterns, high morphological variation, alternations to reproduction, and the depletion of *H. iris* populations, the concern around sustainability of the *H. iris* fishery in NZ is warranted. However, collaborative partnerships between researchers, such as the current study, and the pāua industry (in this case PauaMAC4 and the Pāua Industry Council), provide unique opportunities for developing new management strategies to ensure future growth of pāua populations.

CRediT authorship contribution statement

Joanna S. Copedo: Writing – review & editing, Writing – original draft, Visualization, Methodology, Investigation, Formal analysis, Conceptualization. **Stephen C. Webb:** Writing – review & editing, Supervision. **Lizenn Delisle:** Writing – review & editing, Visualization, Methodology. **Ben Knight:** Writing – review & editing, Visualization, Methodology. **Norman L.C. Ragg:** Writing – review & editing, Supervision, Funding acquisition, Conceptualization. **Olivier Laroche:** Writing – review & editing, Methodology. **Leonie Venter:** Writing – review & editing, Investigation, Conceptualization. **Andrea C. Alfaro:** Writing – review & editing, Supervision, Investigation, Funding acquisition, Conceptualization.

Declaration of competing interest

The authors declare that they have no known competing financial interests or personal relationships that could have appeared to influence the work reported in this paper.

Acknowledgements

This research was funded by the New Zealand Ministry for Business, Innovation and Employment, through the Aquaculture Health Strategies to Maximise Productivity and Security programme (contract CAWX1707) and Cawthron's Shellfish Aquaculture Research Platform (CAWX1801). We offer very special thanks to Tom McCowan, for his support, guidance and reviewing the manuscript. We thank Nick Cameron (PAUMAC4), and Jeremy Cooper (Pāua Industry Council) for logistical support, guidance, and supply of pāua. We also thank the team at Cawthron and the Aquaculture Biotechnology Research Group, AUT, for their intellectual and practical input. Next, we thank Anastasija Zaiko at SeQuench (https://www.sequench.co.nz/contact/) for the metabarcoding sequencing and Jacob Thomson-Liang for his help in the molecular analyses. Finally, thank-you to both Medlab Central, Palmerston North, and Awanui Veterinary Histology for their assistance with histology processing.

Data availability

Data will be made available on request.

References

Aalto, E.A., Barry, J.P., Boch, C.A., Litvin, S.Y., Micheli, F., Woodson, C.B., De Leo, G.A., 2020. Abalone populations are most sensitive to environmental stress effects on adult individuals. Mar. Ecol. Prog. Ser. 643, 75–85. https://www.int-res.com/abstracts/meps/v643/p75-85.

Adema, C.M., 2021. Sticky problems: extraction of nucleic acids from molluscs. Phil. Trans. Roy. Soc. Lond. B Biol. Sci. 376, 20200162. https://doi.org/10.1098/rstb.2020.0162.

Bayne, B.L., 2004. Phenotypic flexibility and physiological tradeoffs in the feeding and growth of marine bivalve molluscs. Integr. Comp. Biol. 44, 425–432. https://doi.org/10.1093/icb/44.6.425.

Behrens, E., Rickard, G., Rosier, S., Williams, J., Morgenstern, O., Stone, D., 2022. Projections of future marine heatwaves for the oceans around New Zealand using New Zealand's earth system model. Frontiers in Climate 4. https://doi.org/10.3389/fclim.2022.798287.

Beninger, P.G., 2017. Caveat observator: the many faces of pre-spawning atresia in marine bivalve reproductive cycles. Mar. Biol. 164, 163. https://doi.org/10.1007/s00227-017-3194-x.

Benson, D.A., Karsch-Mizrachi, I., Lipman, D.J., Ostell, J., Wheeler, D.L., 2008. GenBank. Nucleic Acids Res. 36, D25–D30. https://doi.org/10.1093/nar/gkm929.

Booth, M., 2018. Chapter three - climate change and the neglected tropical diseases. In: Rollinson, D., Stothard, J.R. (Eds.), Advances in Parasitology. Academic Press, pp. 39–126.

Bower, S.M., 2006. Synopsis of Infectious Diseases and Parasites of Commercially Exploited Shellfish: Ciliates Associated with Abalone. Dfo.

Britz, P.J., Hecht, T., Knauer, J., 1996. Gastric evacuation time and digestive enzyme activity in abalone *Haliotis midae* fed a formulated diet. S. Afr. J. Mar. Sci. 17, 297–303. https://doi.org/10.2989/025776196784158581.

Callahan, B.J., McMurdie, P.J., Rosen, M.J., Han, A.W., Johnson, A.J., Holmes, S.P., 2016. DADA2: high-resolution sample inference from Illumina amplicon data. Nat. Methods 13, 581–583. https://doi.org/10.1038/nmeth.3869.

Camacho, C., Coulouris, G., Avagyan, V., Ma, N., Papadopoulos, J., Bealer, K., Madden, T.L., 2009. BLAST+: architecture and applications. BMC Bioinf. 10, 421. https://doi.org/10.1186/1471-2105-10-421.

Carella, F., Aceto, S., Mangoni, O., Mollica, M.P., Cavaliere, G., Trinchese, G., Aniello, F., De Vico, G., 2018. Assessment of the health status of mussels *Mytilus galloprovincialis* along the campania coastal areas: a multidisciplinary approach. Front. Physiol. 9, 683. https://doi.org/10.3389/fphys.2018.00683.

Carella, F.F., Bignell, S.W., DeVico G, J.P., 2015. Comparative pathology in bivalves: etiological agents and disease processes. J. Invertebr. Pathol. 131, 13.

Chérel, D., Beninger, P.G., 2017. Oocyte atresia characteristics and effect on reproductive effort of manila clam *Tapes philippinarum* (adams and reeve, 1850). J. Shellfish Res. 36, 549–557. https://doi.org/10.2983/035.036.0302.

Chin, T.M., Vazquez-Cuervo, J., Armstrong, E.M., 2017. A multi-scale high-resolution analysis of global sea surface temperature. Rem. Sens. Environ. 200, 154–169. https://doi.org/10.1016/j.rse.2017.07.029.

Chong, R.S.-M., 2022. Kidney coccidiosis (scallop, abalone, mussels, oysters, and clams). In: Kibenge, F.S.B., et al. (Eds.), Aquaculture Pathophysiology. Academic Press, pp. 551–553.

Clarke, A., 1988. Seasonality in the antarctic marine environment. Comp. Biochem. Physiol. Part B: Comparative Biochemistry 90, 461–473. https://doi.org/10.1016/0305-0491(88)90285-4.

Cohen, A.A., 2018. Aging across the tree of life: the importance of a comparative perspective for the use of animal models in aging. Biochim. Biophys. Acta, Mol. Basis Dis. 1864, 2680–2689. https://doi.org/10.1016/j.bbadis.2017.05.028.

Cook, P.A., 2014. The worldwide abalone industry. Mod. Econ. 5, 1181–1186. https://doi.org/10.4236/me.2014.513110.

Copedo, J.S., Webb, S.C., Ragg, N.L.C., Ericson, J.A., Venter, L., Schmidt, A.J., Delorme, N.J., Alfaro, A.C., 2023. Histopathological changes in the greenshell

mussel, *Perna canaliculus*, in response to chronic thermal stress. J. Therm. Biol. 117, 103699. https://doi.org/10.1016/j.jtherbio.2023.103699.
Copedo, J.S., Webb, S.C., Ragg, N.L.C., Venter, L., Alfaro, A.C., 2024. Histopathological investigation of four populations of abalone (*Haliotis iris*) exhibiting divergent growth performance. J. Invertebr. Pathol. 202, 108042. https://doi.org/10.1016/j.jip.2023.108042.
Day, R.W., Cook, P., 1995. Bias towards brown algae in determining diet and food preferences: the South African abalone *Haliotis midae*. Mar. Freshw. Res. 46, 623–627. https://doi.org/10.1071/mf9950623.
Delorme, N.J., 2017. Thermal biology of the New Zealand sea urchin. School of Biological science PhD, 160. University of Auckland, Auckland.
Diggles, B.K., Nichol, J., Hin, P.M., Wakefield, S., Cochennec-Laureau, N., Roberts, R.D., Friedman, C.S., 2002. Pathology of cultured paua *Haliotis iris* infected with a novel haplosporidian parasite, with some observations on the course of disease. Dis. Aquat. Org. 50, 219–231. https://doi.org/10.3354/dao050219.
Diggles, B.K., Oliver, M., 2005. Diseases of cultured paua (*Haliotis iris*) in New Zealand. Diseases in Asian Aquaculture 275–287.
Dolman, C.L., MacLeod, P.M., 1981. Lipofuscin and its relation to aging. In: Fedoroff, S., Hertz, L. (Eds.), Advances in Cellular Neurobiology. Elsevier, pp. 205–247.
Fukazawa, H., Takami, H., Kawamura, T., Watanabe, Y., 2005. The effect of egg quality on larval period and postlarval survival of an abalone *Haliotis discus hannai*. J. Shellfish Res. 24, 1141–1147.
Geiger, D.L., 1999. Distribution and biogeography of the recent Haliotidae world-wide: (gastropoda: vetigastropoda). Bollettino Malacologico 57–118.
Gnanalingam, G., Pritchard, D.W., Richards, D.K., Subritzky, P., Flack, B., Hepburn, C.D., 2021. Local management to support local fisheries: Rāhui (temporary closure) and bag limits for Blackfoot abalone (*Haliotis iris*) in southern New Zealand. Aquat. Conserv. Mar. Freshw. Ecosyst. 31, 2320–2333. https://doi.org/10.1002/aqc.3662.
Gordon, H.R., Cook, P.A., 2004. World abalone fisheries and aquaculture update: supply and market dynamics. J. Shellfish Res. 23, 935–940.
Hadfield, J.D., 2010. MCMC methods for multi-response generalized linear mixed models: TheMCMCglmmRPackage. J. Stat. Software 33, 1–22. https://doi.org/10.18637/jss.v033.i02.
Halpern, B.S., Walbridge, S., Selkoe, K.A., Kappel, C.V., Micheli, F., D'Agrosa, C., Bruno, J.F., Casey, K.S., Ebert, C., Fox, H.E., Fujita, R., Heinemann, D., Lenihan, H.S., Madin, E.M., Perry, M.T., Selig, E.R., Spalding, M., Steneck, R., Watson, R., 2008. A global map of human impact on marine ecosystems. Science 319, 948–952. https://doi.org/10.1126/science.1149345.
Handlinger, J., 2022. General pathology and diseases of abalone. In: Kibenge, F.S.B., et al. (Eds.), Aquaculture Pathophysiology. Academic Press, pp. 405–447.
Handlinger, J., Bastianello, S., Callinan, R., Carson, J., Creeper, J., Deveney, M., Forsyth, W., Freeman, K., Hooper, C., Jones, B., 2002. Abalone aquaculture subprogram: a national survey of diseases of commercially exploited abalone species to support trade and translocation issues and the development of health surveillance programs. FRDC project Report 201.
Hine, P.M., 1997. Health Status of Commercially Important Molluscs in New Zealand. Ministry for Primary Industries.
Hine, P.M., Wakefield, S., Diggles, B.K., Webb, V.L., Maas, E.W., 2002. Ultrastructure of a haplosporidian containing Rickettsiae, associated with mortalities among cultured paua *Haliotis iris*. Dis. Aquat. Org. 49, 207–219. https://doi.org/10.3354/dao049207.
Hole, L.M., Moore, M.N., Bellamy, D., 1995. Age-related cellular and physiological reactions to hypoxia and hyperthermia in marine mussels. Mar. Ecol. Prog. Ser. 122, 173–178. https://ezproxy.aut.ac.nz/login?url=https://search.ebscohost.com/login.aspx?direct=true&site=eds-live&db=edsjsr&AN=edsjsr.24852267.
Hooper, C., Day, R., Slocombe, R., Benkendorff, K., Handlinger, J., Goulias, J., 2014. Effects of severe heat stress on immune function, biochemistry and histopathology in farmed Australian abalone (hybrid Haliotis laevigata×Haliotis rubra). Aquaculture 432, 26–37. https://doi.org/10.1016/j.aquaculture.2014.03.032.
Houghton, J.E.T., Ding, Y., Griggs, D., Noguer, M., van der Linden, P., Dai, X., Maskell, M., Johnson, C., 2001. Climate Change 2001: the Scientific Basis: Contribution of Working Group I to the Third Assessment Report of the Intergovernmental Panel on Climate Change (IPCC). Cambridge University Press, p. 881.
Howard, D.W., 2004. Histological techniques for marine bivalve mollusks and crustaceans. In: NOAA, National Ocean Service, National Centers for Coastal Ocean Service, Center for Coastal Environmental Health and Biomolecular Research. Cooperative Oxford Laboratory.
JPL, DAAC, 2015. GHRSST level 4 MUR global foundation Sea Surface temperature analysis. In: DAAC, P.O. (Ed.), JPL MUR MEaSUREs Project. CA, USA.
Jung, T., Bader, N., Grune, T., 2007a. Lipofuscin: formation, distribution, and metabolic consequences. Ann. N. Y. Acad. Sci. 1119, 97–111. https://doi.org/10.1196/annals.1404.008.
Jung, T., Bader, N., Grune, T., 2007b. Lipofuscin: formation, distribution, and metabolic consequences. Ann. N. Y. Acad. Sci. 1119, 97–111. https://doi.org/10.1196/annals.1404.008.
Kim, H., Kim, B.H., Son, M.H., Jeon, M.A., Lee, Y.G., Lee, J.S., 2016. Gonadal development and reproductive cycle of cultured abalone, *Haliotis discus hannai,* (gastropoda: Haliotidae) in korea: implications for seed production. J. Shellfish Res. 35, 653–659. https://doi.org/10.2983/035.035.0311, 7.
Knowles, G., Handlinger, J., Jones, B., Moltschaniwskyj, N., 2014. Hemolymph chemistry and histopathological changes in Pacific oysters (*Crassostrea gigas*) in response to low salinity stress. J. Invertebr. Pathol. 121, 78–84. https://doi.org/10.1016/j.jip.2014.06.013.
Kooijman, B., Kooijman, S., 2010. Dynamic Energy Budget Theory for Metabolic Organisation. Cambridge university press.
Laferriere, A.A.M., 2016. Examining the Ecological Complexities of Blackfoot Paua Demography and Habitat Requirements in the Scope of Marine Reserve Protection, Doctorate. Victoria University of Wellington, Victoria University of Wellington.
Lane, H.S., Jaramillo, D., Sharma, M., 2023. *Perkinsus olseni* in green-lipped mussels *Perna canaliculus*: diagnostic evaluation, prevalence, and distribution. Dis. Aquat. Org. 155, 175–185. https://doi.org/10.3354/dao03750.
Laroche, O., 2024. biohelper: bioinformatics and data analysis helper functions (0.0.11.000). https://rdrr.io/github/olar785/biohelper/.
Lenth, R.V., 2021. Emmeans: estimated marginal means, aka least-squares means. https://CRAN.R-project.org/package=emmeans.
Lima, F.P., Wethey, D.S., 2012. Three decades of high-resolution coastal sea surface temperatures reveal more than warming. Nat. Commun. 3, 704. https://doi.org/10.1038/ncomms1713.
Liu, G., Heron, S.F., Eakin, C.M., Muller-Karger, F.E., Vega-Rodriguez, M., Guild, L.S., De La Cour, J.L., Geiger, E.F., Skirving, W.J., Burgess, T.F.R., Strong, A.E., Harris, A., Maturi, E., Ignatov, A., Sapper, J., Li, J., Lynds, S., 2014. Reef-scale thermal stress monitoring of coral ecosystems: new 5-km global products from NOAA coral reef Watch. Remote Sens. 6, 11579–11606. https://www.mdpi.com/2072-4292/6/11/11579.
Lleonart, M., 1992. A Gonad Conditioning Study of the Greenlip Abalone (*Haliotis Laevigata*), Masters. University of Tasmania, p. 162.
Lotze, H.K., Lenihan, H.S., Bourque, B.J., Bradbury, R.H., Cooke, R.G., Kay, M.C., Kidwell, S.M., Kirby, M.X., Peterson, C.H., Jackson, J.B., 2006. Depletion, degradation, and recovery potential of estuaries and coastal seas. Science 312, 1806–1809. https://doi.org/10.1126/science.1128035.
Mai, K., Mercer, J.P., Donlon, J., 1995. Comparative studies on the nutrition of two species of abalone, *Haliotis tuberculata* L. and *Haliotis discus hannai* Ino. III. response of abalone to various levels of dietary lipid. Aquaculture 134, 65–80. https://doi.org/10.1016/0044-8486(95)00043-2.
Marigomez, I., Soto, M., Cajaraville, M.P., Angulo, E., Giamberini, L., 2002. Cellular and subcellular distribution of metals in molluscs. Microsc. Res. Tech. 56, 358–392. https://doi.org/10.1002/jemt.10040.
Martin, M., 2011. Cutadapt removes adapter sequences from high-throughput sequencing reads. EMBnet.journal. 17 (3). https://doi.org/10.14806/ej.17.1.200.
McAvaney, L.A., Day, R.W., Dixon, C.D., Huchette, S.M., 2004. Gonad development in seeded *Haliotis laevigata*: growth environment determines initial reproductive investment. J. Shellfish Res. 23, 1213–1218.
McShane, P.E., Schiel, D.R., Mercer, S.F., Murray, T., 1994. Morphometric variation in *Haliotis iris* (Mollusca: gastropoda): analysis of 61 populations. N. Z. J. Mar. Freshw. Res. 28, 357–364.
Miller, M.A., Zachary, J.F., 2017. Chapter 1 Mechanisms and Morphology of Cellular Injury, Adaptation, and Death 1 1 for a Glossary of Abbreviations and Terms Used in This Chapter See E-Glossary 1-1. Pathologic Basis of Veterinary Disease.
Montie, S., Thoral, F., Smith, R.O., Cook, F., Tait, L.W., Pinkerton, M.H., Schiel, D.R., Thomsen, M.S., 2023. Seasonal trends in marine heatwaves highlight vulnerable coastal ecoregions and historic change points in New Zealand. N. Z. J. Mar. Freshw. Res. 58, 274–299. https://doi.org/10.1080/00288330.2023.2218102.
Morash, A.J., Alter, K., 2016. Effects of environmental and farm stress on abalone physiology: perspectives for abalone aquaculture in the face of global climate change. Rev. Aquacult. 8, 342–368. https://doi.org/10.1111/raq.12097.
Moss, G.A., 1998. Effect of temperature on the breeding cycle and spawning success of the New Zealand abalone, *Haliotis australis*. N. Z. J. Mar. Freshw. Res. 32, 139–146. https://doi.org/10.1080/00288330.1998.9516813.
Mpi, M.f.P.I., 2023a. Pāua status and information. https://www.mpi.govt.nz/fishing-aquaculture/recreational-fishing/information-on-popular-fish-in-nz/paua-status-and-information/.
Mpi, M.f.P.I., 2023b. Recreational daily pāua limits reduced for lower and central North Island. https://www.mpi.govt.nz/news/media-releases/recreational-daily-paua-limits-reduced-for-lower-and-central-north-island/#:~:text=The%20daily%20limit%20for%20recreationally,effect%20on%204%20September%202023.
Muznebin, F., Alfaro, A.C., Webb, S.C., 2021. Occurrence of *Perkinsus olseni* and other parasites in New Zealand black-footed abalone (*Haliotis iris*). N. Z. J. Mar. Freshw. Res. 57, 261–281. https://doi.org/10.1080/00288330.2021.1984950.
Naylor, J.R., Andrew, N.L., Kim, S.W., 2006. Demographic variation in the New Zealand abalone *Haliotis iris*. Mar. Freshw. Res. 57, 215–224.
Nguyen, T.T., Marsden, I.D., Davison, W., Pirker, J., 2023. Effects of acclimation temperature and exposure time on the scope for growth of the Blackfoot Pāua (*Haliotis iris*). Mar. Freshw. Res. 74, 1465–1477.
Nguyen, T.V., Alfaro, A., Frost, E., Chen, D., Beale, D.J., Mundy, C., 2021. Investigating the biochemical effects of heat stress and sample quenching approach on the metabolic profiling of abalone (*Haliotis iris*). Metabolomics 18 (7). https://doi.org/10.1007/s11306-021-01862-8.
Pāua Industry Council, 2023. Markets and exports. https://www.paua.org.nz/markets-export.
Perez-Cebrecos, M., Prieto, D., Blanco-Rayon, E., Izagirre, U., Ibarrola, I., 2022. Differential tissue development compromising the growth rate and physiological performances of mussel. Mar. Environ. Res. 180, 105725. https://doi.org/10.1016/j.marenvres.2022.105725.
Pérez, A.F., Boy, C.C., Curelovich, J.N., Pérez Barros, P., Calcagno, J.Á., 2013. Relationship between Energy Allocation and Gametogenesis in *Aulacomya Atra* (Bivalvia: Mytilidae) in a Sub-antarctic Environment, vol. 48, pp. 459–469.
Petes, L.E., Menge, B.A., Murphy, G.D., 2007. Environmental stress decreases survival, growth, and reproduction in New Zealand mussels. J. Exp. Mar. Biol. Ecol. 351, 83–91.

Philipp, E., Brey, T., Portner, H.O., Abele, D., 2005. Chronological and physiological ageing in a polar and a temperate mud clam. Mech. Ageing Dev. 126, 598–609. https://doi.org/10.1016/j.mad.2004.12.003.
Poore, G.C.B., 1972. Ecology of New Zealand abalones, *haliotis* species (Mollusca: gastropoda). N. Z. J. Mar. Freshw. Res. 6, 11–22. https://doi.org/10.1080/00288330.1977.9515407.
Poore, G.C.B., 1973. Ecology of New Zealand abalones, *Haliotis* species (Mollusca: gastropoda). N. Z. J. Mar. Freshw. Res. 7, 67–84. https://doi.org/10.1080/00288330.1973.9515456.
Portner, H.O., Farrell, A.P., 2008. Ecology. Physiology and climate change. Science 322, 690–692. https://doi.org/10.1126/science.1163156.
Quast, C., Pruesse, E., Yilmaz, P., Gerken, J., Schweer, T., Yarza, P., Peplies, J., Glockner, F.O., 2013. The SILVA ribosomal RNA gene database project: improved data processing and web-based tools. Nucleic Acids Res. 41, D590–D596. https://doi.org/10.1093/nar/gks1219.
R Core Team, 2024. R: A Language and Environment for Statistical Computing. R Foundation for Statistical Computing. https://www.R-project.org/.
Ragg, N.L.C., 2023. Physiology: energetics, metabolism, and gas exchange. In: Cook, P. A., Shumway, S.E. (Eds.), Abalone: Biology, Ecology, Aquaculture and Fisheries. Elsevier, pp. 119–160.
Rajapandi, T., 2020. Apicomplexan lineage-specific polytopic membrane proteins in Cryptosporidium parvum. J. Parasit. Dis. 44, 467–471. https://doi.org/10.1007/s12639-020-01209-5.
Reece, K.S., Stokes, N.A., 2003. Molecular analysis of a haplosporidian parasite from cultured New Zealand abalone *Haliotis iris*. Dis. Aquat. Org. 53, 61–66. https://doi.org/10.3354/dao053061.
Ren, J.S., Fox, S.P., Howard-Williams, C., Zhang, J., Schiel, D.R., 2019. Effects of stock origin and environment on growth and reproduction of the green-lipped mussel *Perna canaliculus*. Aquaculture 505, 502–509. https://doi.org/10.1016/j.aquaculture.2019.03.011.
Rogers-Bennett, L., Catton, C.A., 2019. Marine heat wave and multiple stressors tip bull kelp forest to sea urchin barrens. Sci. Rep. 9, 15050. https://doi.org/10.1038/s41598-019-51114-y.
Rogers-Bennett, L., Dondanville, R.F., Moore, J.D., Vilchis, L.I., 2010. Response of red abalone reproduction to warm water, starvation, and disease stressors: implications of ocean warming. J. Shellfish Res. 29, 599–611. https://doi.org/10.2983/035.029.0308, 13.
Rogers-Bennett, L., Klamt, R., Catton, C.A., 2021. Survivors of climate driven abalone mass mortality exhibit declines in health and reproduction following kelp forest collapse. Front. Mar. Sci. 8. https://doi.org/10.3389/fmars.2021.725134.
Roussel, S., Huchette, S., Gaillard, F., Servili, A., Malet, L., Di Giglio, S., Richard, N., Coheleach, M., Badou, A., Dubois, P., Martin, S., Auzoux-Bordenave, S., Avignon, S., Norkko, J., 2020. An integrated investigation of the effects of ocean acidification on adult abalone (*Haliotis tuberculata*). ICES (Int. Counc. Explor. Sea) J. Mar. Sci. 77, 757–772. https://doi.org/10.1093/icesjms/fsz257.
RStudio Team, 2021. RStudio: integrated development environment for R. http://www.rstudio.com/.
Sainsbury, K.J., 2010. Population dynamics and fishery management of the paua, *Haliotis iris*. Population structure, growth, reproduction, and mortality. N. Z. J. Mar. Freshw. Res. 16, 147–161. https://doi.org/10.1080/00288330.1982.9515958.
Salinger, M.J., Diamond, H.J., Behrens, E., Fernandez, D., Fitzharris, B.B., Herold, N., Johnstone, P., Kerckhoffs, H., Mullan, A.B., Parker, A.K., Renwick, J., Scofield, C., Siano, A., Smith, R.O., South, P.M., Sutton, P.J., Teixeira, E., Thomsen, M.S., Trought, M.C.T., 2020. Unparalleled coupled ocean-atmosphere summer heatwaves in the New Zealand region: drivers, mechanisms and impacts. Clim. Change 162, 485–506. https://doi.org/10.1007/s10584-020-02730-5.
Santana-Falcón, Y., Séférian, R., 2022. Climate change impacts the vertical structure of marine ecosystem thermal ranges. Nat. Clim. Change 12, 935–942. https://doi.org/10.1038/s41558-022-01476-5.
Saulsbury, J., Moss, D.K., Ivany, L.C., Kowalewski, M., Lindberg, D.R., Gillooly, J.F., Heim, N.A., McClain, C.R., Payne, J.L., Roopnarine, P.D., Schöne, B.R., Goodwin, D., Finnegan, S., 2019. Evaluating the influences of temperature, primary production, and evolutionary history on bivalve growth rates. Paleobiology 45, 405–420. https://doi.org/10.1017/pab.2019.20.
Saunders, T.M., Connell, S.D., Mayfield, S., 2009. Differences in abalone growth and morphology between locations with high and low food availability: morphologically fixed or plastic traits? Mar. Biol. 156, 1255–1263.
Saunders, T.M., Mayfield, S., Hogg, A.A., 2008. A simple, cost-effective, morphometric marker for characterising abalone populations at multiple spatial scales. Mar. Freshw. Res. 59, 32–40. https://doi.org/10.1071/mf07150.
Schiel, D.R., 1993. Experimental evaluation of commercial-scale enhancement of abalone *Haliotis iris* populations in New Zealand. Mar. Ecol. Prog. Ser. 97, 167–181. https://ezproxy.aut.ac.nz/login?url=https://search.ebscohost.com/login.aspx?direct=true&site=eds-live&db=edsjsr&AN=edsjsr.24833613.
Schiel, D.R., Wood, S.A., Dunmore, R.A., Taylor, D.I., 2006. Sediment on rocky intertidal reefs: effects on early post-settlement stages of habitat-forming seaweeds. J. Exp. Mar. Biol. Ecol. 331, 158–172. https://doi.org/10.1016/j.jembe.2005.10.015.
Schoch, C.L., Ciufo, S., Domrachev, M., Hotton, C.L., Kannan, S., Khovanskaya, R., Leipe, D., McVeigh, R., O'Neill, K., Robbertse, B., Sharma, S., Soussov, V., Sullivan, J.P., Sun, L., Turner, S., Karsch-Mizrachi, I., 2020. NCBI Taxonomy: a comprehensive update on curation, resources and tools. Database 2020. https://doi.org/10.1093/database/baaa062.
Searle, T., Roberts, R.D., Lokman, P.M., 2006. Effects of temperature on growth of juvenile Blackfoot abalone, *Haliotis iris* Gmelin. Aquac. Res. 37, 1441–1449.
Seehafer, S.S., Pearce, D.A., 2006. You say lipofuscin, we say ceroid: defining autofluorescent storage material. Neurobiol. Aging 27, 576–588. https://doi.org/10.1016/j.neurobiolaging.2005.12.006.
Shaw, J.P., Moore, M.N., Readman, J.W., Mou, Z., Langston, W.J., Lowe, D.M., Frickers, P.E., Al-Moosawi, L., Pascoe, C., Beesley, A., 2019. Oxidative stress, lysosomal damage and dysfunctional autophagy in molluscan hepatopancreas (digestive gland) induced by chemical contaminants. Mar. Environ. Res. 152, 104825. https://doi.org/10.1016/j.marenvres.2019.104825.
Shin, S.R., Kim, H.J., Lee, D.H., Kim, H., Sohn, Y.C., Kim, J.W., Lee, J.S., 2020. Gonadal maturation and main spawning period of *Haliotis gigantea* (gastropoda: Haliotidae). Dev Reprod 24, 79–88. https://doi.org/10.12717/DR.2020.24.2.79.
Smale, D.A., Wernberg, T., Oliver, E.C.J., Thomsen, M., Harvey, B.P., Straub, S.C., Burrows, M.T., Alexander, L.V., Benthuysen, J.A., Donat, M.G., Feng, M., Hobday, A. J., Holbrook, N.J., Perkins-Kirkpatrick, S.E., Scannell, H.A., Sen Gupta, A., Payne, B. L., Moore, P.J., 2019. Marine heatwaves threaten global biodiversity and the provision of ecosystem services. Nat. Clim. Change 9, 306–312. https://doi.org/10.1038/s41558-019-0412-1.
Sokolova, I.M., Frederich, M., Bagwe, R., Lannig, G., Sukhotin, A.A., 2012. Energy homeostasis as an integrative tool for assessing limits of environmental stress tolerance in aquatic invertebrates. Mar. Environ. Res. 79, 1–15. https://doi.org/10.1016/j.marenvres.2012.04.003.
Soon, T.K., Ransangan, J., 2019. Extrinsic factors and marine bivalve mass mortalities: an overview. J. Shellfish Res. 38, 223–232. https://doi.org/10.2983/035.038.0202, 10.
Srisuphanunt, M., Wilairatana, P., Kooltheat, N., Damrongwatanapokin, T., Karanis, P., 2023. Occurrence of Cryptosporidium oocysts in commercial oysters in southern Thailand. Food Waterborne Parasitol 32, e00205. https://doi.org/10.1016/j.fawpar.2023.e00205.
Srisuphanunt, M., Wiwanitkit, V., Saksirisampant, W., Karanis, P., 2009. Detection of Cryptosporidium oocysts in green mussels (*Perna viridis*) from shell-fish markets of Thailand. Parasite 16, 235–239. https://doi.org/10.1051/parasite/2009163235.
Steele, S., Mulcahy, M., 1999. Gametogenesis of the oyster *Crassostrea gigas* in southern Ireland. J. Mar. Biol. Assoc. U. K. 79, 673–686.
Steeves, L., Filgueira, R., Guyondet, T., Chassé, J., Comeau, L., 2018. Past, present, and future: performance of two bivalve species under changing environmental conditions. Front. Mar. Sci. 5, 184. https://doi.org/10.3389/fmars.2018.00184.
Steffani, C.N., Branch, G.M., 2003. Growth rate, condition, and shell shape of *Mytilus galloprovincialis*: responses to wave exposure. Mar. Ecol. Prog. Ser. 246, 197–209. https://doi.org/10.3354/meps246197.
Stuart, M.D., Brown, M.T., 1994. Growth and diet of cultivated black-footed abalone, *Haliotis iris* (Martyn). Aquaculture 127, 329–337. https://doi.org/10.1016/0044-8486(94)90235-6.
Subritzky, P., 2013. The Identification of Juvenile *Haliotis Iris* Habitat within the East Otago Taiāpure. University of Otago.
Terman, A., Brunk, U.T., 1998. Lipofuscin: mechanisms of formation and increase with age. Apmis 106, 265–276. https://doi.org/10.1111/j.1699-0463.1998.tb01346.x.
Thomas, L.J., Milotic, M., Vaux, F., Poulin, R., 2022. Lurking in the water: testing eDNA metabarcoding as a tool for ecosystem-wide parasite detection. Parasitology 149, 261–269. https://doi.org/10.1017/S0031182021001840.
Thomsen, M.S., Mondardini, L., Alestra, T., Gerrity, S., Tait, L., South, P.M., Lilley, S.A., Schiel, D.R., 2019. Local extinction of bull kelp (*durvillaea* spp.) due to a marine heatwave. Front. Mar. Sci. 6. https://doi.org/10.3389/fmars.2019.00084.
Trussell, G.C., 1996. Phenotypic plasticity in an intertidal snail: the role of a common crab predator. Evolution 50, 448–454. https://doi.org/10.1111/j.1558-5646.1996.tb04507.x.
Van Nguyen, T., Alfaro, A.C., Venter, L., Ericson, J.A., Ragg, N.L.C., McCowan, T., Mundy, C., 2023. Metabolomics approach reveals size-specific variations of Blackfoot abalone (*Haliotis iris*) in Chatham Islands, New Zealand. Fish. Res. 262, 106645. https://doi.org/10.1016/j.fishres.2023.106645.
Vélez-Arellano, N., García-Domínguez, F.A., Lluch-Cota, D.B., Gutiérrez-González, J.L., Sánchez-Cárdenas, R., 2015. Histological validation of morphochromatically-defined gonadal maturation stages of green abalone (*Haliotis fulgens*) Philippi,1845 and pink abalone (*Haliotis corrugata*) wood, 1828. Int. J. Morphol. 33, 1054–1059. https://doi.org/10.4067/s0717-95022015000300039.
Venables, B., Ripley, B., 2002. Modern Applied Statistics with S.
Venter, L., Alfaro, A.C., Van Nguyen, T., Lindeque, J.Z., 2022. Metabolite profiling of abalone (*Haliotis iris*) energy metabolism: a Chatham Islands case study. Metabolomics 18, 52. https://doi.org/10.1007/s11306-022-01907-6.
Viera, M.P., de Vicose, G.C., Gómez-Pinchetti, J.L., Bilbao, A., Fernandez-Palacios, H., Izquierdo, M.S., 2011. Comparative performances of juvenile abalone (*Haliotis tuberculata coccinea* Reeve) fed enriched vs non-enriched macroalgae: effect on growth and body composition. Aquaculture 319, 423–429. https://doi.org/10.1016/j.aquaculture.2011.07.024.
Wang, Q., Garrity, G.M., Tiedje, J.M., Cole, J.R., 2007. Naive Bayesian classifier for rapid assignment of rRNA sequences into the new bacterial taxonomy. Appl. Environ. Microbiol. 73, 5261–5267. https://doi.org/10.1128/AEM.00062-07.
Webb, S.C., Duncan, J., 2019. New Zealand Shellfish Health Monitoring 2007 to 2017: Insights and Projections. Cawthron Report No. 2568. 67.
Webber, H., Giese, A., 1969. Reproductive cycle and gametogenesis in the black abalone *Haliotis cracherodii* (Gastropoda: prosobranchiata). Mar. Biol. 4, 152–159.

Wilson, N.H.F., Schiel, D.R., 1995. Reproduction on two species of abalone (*Haliotis iris* and *H. australis*) in southern New Zealand. Mar. Freshw. Res. 46, 629–637. https://doi.org/10.1071/mf9950629.

Zaroogian, G., Yevich, P., 1993. Cytology and biochemistry of brown cells in *Crassostrea virginica* collected at clean and contaminated stations. Environ. Pollut. 79, 191–197. https://doi.org/10.1016/0269-7491(93)90069-z.

Zhan, A., Hulák, M., Sylvester, F., Huang, X., Adebayo, A.A., Abbott, C.L., Adamowicz, S. J., Heath, D.D., Cristescu, M.E., MacIsaac, H.J., 2013. High sensitivity of 454 pyrosequencing for detection of rare species in aquatic communities. Methods Ecol. Evol. 4, 558–565.